MASTER OF SCIENCE BY RESEARCH

A new SPR fatigue estimation method for aluminium car body

Thomas Varghese, Robin

Award date:
2011

Awarding institution:
Coventry University

A New SPR Fatigue Estimation Method for Aluminium Car Body

By

Robin Thomas Varghese

September 2011

A thesis submitted in partial fulfilment of the University's requirements for the Degree of Masters by Research

Declaration

I declare that in submitting this work:

- I am aware of no health reasons that will prevent me from undertaking and completing the assessment, and will undertake notifying my Director of Studies and Registry Research Unit as soon as any change in these circumstances occurs."
- That it is my own work and does not involve plagiarism, other forms of cheating or the unattributed work of other people.

Robin Thomas Varghese 16/09/11

SID: 1560851

DoS:

Dr Paul Briskham

Department of EKM

Faculty of Engineering and Computing

Acknowledgement

I would like to thank my supervisor Dr Paul Briskham, for giving me the chance to pursue this research under his supervision. I would also like to thank Andrew Blows and Tim Mumford of Jaguar Cars, and Peter Heyes of HBM, for the opportunity they gave me to work with them through this research, at its various stages. I would like to thank Dr John Karadelis of the Civil Engineering Department of Coventry University for his insights. I would also like to thank my second supervisor Dr Phil Swanson, for his support and input. Finally I would like thank my friends and family for their unwavering support through the course of this research.

Abstract

The thesis consists of an analysis of spot joint fatigue estimation models suitable for aluminium car body. The gaps were identified in the existing models and a new approach put forth for SPR fatigue estimation, with a body in white validation plan. In the process, SPR fatigue failure mechanisms were also analysed. The models were critically analysed, including the proposed one. Fatigue as a phenomenon and its perception in the automotive industry were also discussed. Avenues of future work were identified and discussed briefly.

Contents

Table of Figures

1. Introduction

The introductory chapter has the following objectives:

1. To introduce the reader to the phenomenon of fatigue and some of its aspects.

2. Introduce a relatively new and preferred joining technique - self piercing rivets.

1.1 Fatigue

Fatigue as the term suggests is an accumulation of damage over time which leads to an apparently abrupt or sudden failure of a component or material. In the report entitled *General Principles for Fatigue Testing of Metals* published by International Organisation for Standardization in Geneva in 1964 the term fatigue is referred to as 'Changes in properties which can occur in a metallic material due to repeated application of stresses and strains.' (Suresh, 2004 p1). These changes lead ultimately to failure.

It can also be defined as:

- Failure under repeated or otherwise varying load which never reaches a level close to failure in a single application. (Bishop and Sherratt, 2000 p5)
- A form of failure that occurs in structures subjected to dynamic and fluctuating stresses under circumstances where it is possible for failure to occur at a stress level considerably lower that the tensile or yield strength for a static load. (Callister, 2007 p227)
- Damage or failure of materials under cyclic loads. (Suresh, 2004 p1)

The importance of fatigue lies in that it is believed to be the single largest cause of metal failure. 50- 90% of all metal failures are believed to be due to fatigue (Stephens et al., 2001

p3), (Callister, 2007 p227), (Gokhale et al., 2008 p295), (Manson and Halford, 2006 p1), (Liguore and Beier, 2001 p1). It has been established that fatigue failure takes place in stages (Grinberg, 1984 p229), (Hamano, 1997 p197), (Yang et al., 2001 p52), (Verdu et al., 2008). The entire process may consist of as many as 5 stages: (De-Guang et al., 1998 p683), (Xue et al., 2007 p2812), (Suresh, 2004 p11)

1) Early cyclic formation and micro-structural changes
2) Micro-crack nucleation
3) Micro-crack propagation
4) Macro-crack propagation
5) Final critical failure leading to structural instability

Indispensably, the early stages of fatigue is of paramount interest and importance for safety as well as robustness of structures (Papazian et al., 2007 p1668), (Yang et al., 2001 p51).

Fatigue is probabilistic and a deterministic value cannot be attributed to fatigue life.

1.2 Fatigue estimation methodologies

In general and in broad terms, there are three major methodologies for estimation of fatigue life. Their use is based on the functionality, geometry and material properties of the component under fatigue. (Bishop and Sherratt, 2000) They are:

1. Stress Life Methodology
2. Strain Life Methodology
3. Fracture Mechanics

1.2.1 Stress Life Methodology

This methodology is considered appropriate for applications where the majority of the desired fatigue life of the material falls within the elastic limit of the life of the material. This methodology is preferred for spot joints in automotive structures. The construction and use of a fatigue estimation model based on this methodology for spot joints in car body could be a complex process. But for a conceptual understanding, fatigue estimation using this methodology may be simplified as involving the following steps:

1. Calculating the fatigue life of the joint through lab tests, using specific joint configuration and material. It may be noted again that the fatigue life of any material or component is not a deterministic value. Therefore, an absolute number cannot be attributed to it. The common practice is to conduct a series of fatigue tests at different load levels, so a mean fatigue life at different load levels may be arrived at.

2. Converting the forces in step 1 into stresses based on equations, and thus generating a stress-life curve. The equations may be derived keeping in mind the following:

    a. The geometry of the joint

    b. The critical locations of stress concentration, as failures are believed to originate from these locations

    c. The key forces that contribute to the creation of the stress concentration location(s), in light of the geometry of the joint, and the forces applied on them.

3. Identifying the forces and (or) moments passing through the critical joint locations of the car body, through Finite Element analysis.

4. Converting these forces and (or) moments to their appropriate stresses using the derived equations mentioned in step 2.

5. Using the stress life curve of the component, attributing a life to the critical joints.

It may be noted again that the points mentioned above constitute the basic conceptual building blocks for a fatigue estimation model using stress life methodology. Complexities and various other considerations arise based on factors, some of which are enlisted as follows:

- Geometric complexities of joints
- Load cycle complexities/variations
- Material batches joint samples
- Laboratory test parameters
- Surface treatment of the materials
- Test coupon configurations

1.2.2 Strain Life Methodology

This methodology is preferred for applications where a considerable amount of the fatigue life is outside the elastic regime of the component. This method is used in components that consist of notches or other stress concentration locations that undergo some plastic

deformation under load, but do not fail as the material around these locations of plastic deformation tends to remain within the elastic range. The steps involved in the construction of a fatigue estimation model based on this methodology include conducting a strain controlled fatigue test of the material undergoing plastic deformation, to generate a strain life curve.

In automotive structures, stiffness of the car body is an important design criterion (Helmut et al., 2004). Therefore, any plastic deformation in the spot joint during load cycles may be argued as a failure of the joint, especially with mechanical joints like self piercing rivets. The majority of the desired fatigue life in such applications lies within the elastic regime. Thus, stress life methodology may be preferred over strain life methodology for spot joints in automotive structures. However, strain life method may be preferred in estimating the fatigue life of structural notches.

1.2.3 Fracture Mechanics Methodology

This methodology is preferred for applications that involve the propagation of a crack or failure for the majority of the desired fatigue life. The crack propagation rates are experimentally determined. This methodology has been used for the fatigue estimation of bonded joints. It assumes the pre-existence of a crack of certain length in the joint.

A healthy spot joint may not be ideally believed to have a crack to start with. For spot joints in automotive applications with stiffness requirements, a stress life or a strain life approach may be preferred over a fracture mechanics approach.

1.3 Fatigue in automotive structures

It is vital for the automotive industry to build durable automotive structures for safety and long term customer satisfaction. Therefore, in automotive structural applications fatigue performance is an indispensable design consideration (Herrmann et al., 2005 p1), (Fatemi and Zoroufi, 2005). Its indispensability becomes even more important as there is a preference toward use of light weight materials in the car body structure for better fuel economy. The move towards increased use of light weight materials has led to the elevation of aluminium as a possible light weight replacement for steel in the car body structure. The car body represents a large fraction of mass (about 27%) in a standard high volume car and the use of aluminium instead of steel can reduce the body mass by about 40%. (Graeve and Zengen, 2009 p3), (Shibata et al., 2003 p939), (Kelkar et al., 2001).

With the advent of the use of new material for car bodies, the need for developing new joining techniques and their evaluation also arises (Sun et al., 2006 p370), (Briskham et al., 2006 p1). A lack of appropriate evaluation of any new joining technique, coupled with the need for endurance would lead to over-engineering, which leads to higher cost.

1.4. Self Piercing Rivets

Self piercing rivets (SPR) are being considered as a favourable joining technique for joining aluminium body panels due to a number of reasons pointed out by both academic and industrial researchers. The primary and major benefits of using SPR are summarised as follows: (Agrawal et al., 2003 p1), (Dannbauer et al., 2003 p1), (Chen et al., 2003 p1), (Han et al., 2007 p1), (Fu and Mallick, 2001p1), (Han and Chrysanthou, 2007 p458), (Atzeni et al., 2009 p1), (Sun et al., 2006 p370), (Iyer et al., 2005 p1), (Han et al., 2006 p1), (Casalino et al., 2008 p787), (Johnson et al., 2009 p662), (He et al., 2008 p28), (Abe et al., 2009 p3921)

- Relatively quiet and simple process
- Easy to automate
- Does not produce fume or spatter
- Requires less power
- Can be used to join a range of materials with a range of thicknesses with a range of coatings or no coating
- The joints are more consistent compared to spot welds
- Posses superior fatigue properties compared to conventional spot welds
- Can be used with structural adhesives to give hybrid joints

SPR is a mechanical joining process where a rivet pierces the top sheet and any middle sheet and deforms in the bottom sheet under the influence of a die thereby locking the sheets together. Figure 1 is a cross-section of an SPR joining a 2 mm top sheet to a 3 mm bottom sheet. Figure 2 shows a schematic sketch of the joining process. The SPR joining process makes use of the following elements:

- Hydraulic or servo electric actuator
- Clamp with an inner concentric punch
- Die

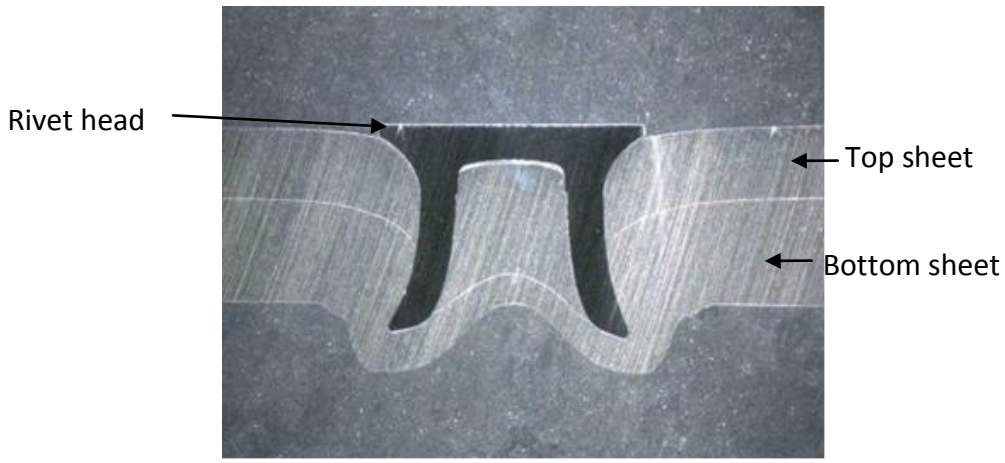

Figure 1: SPR Cross section

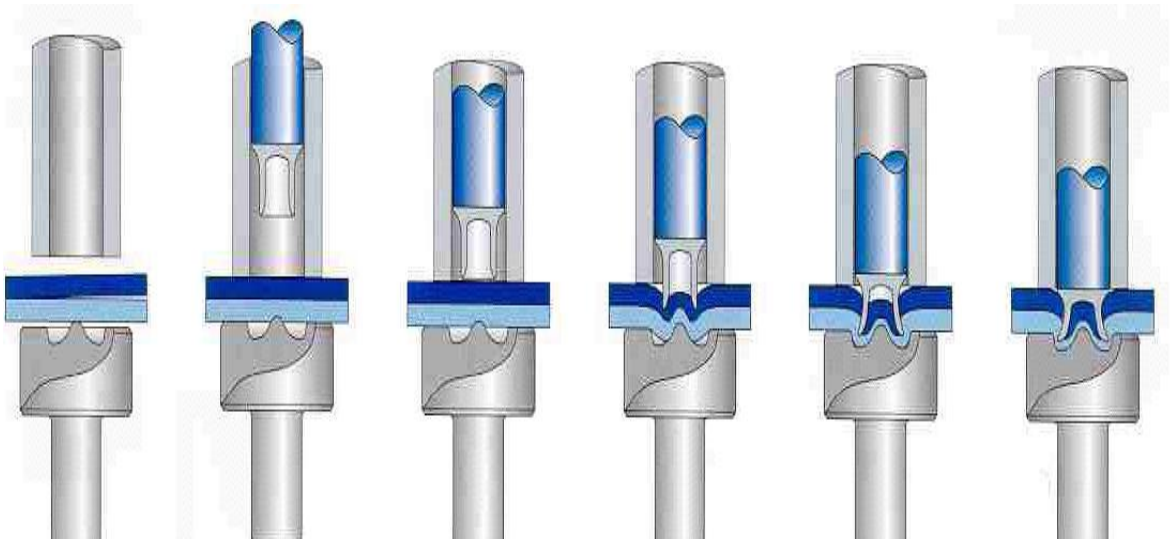

Figure 2: Schematic of SPR joining process

The clamp and punch connected to an actuator is on the head side of the sheets to be joint and the die is on the button side. The sheets to be joint are clamped under a typical clamping pressure of 100 bar (Blackmore, 2007 p2). The punch is then actuated with a pressure of around 240 bar for a servo-hydraulic actuator forcing the rivet legs through the top sheet and not fully through the bottom sheet under the influence of a die. The rivet and die dimensions are pre-calculated and determined for appropriate sheet thicknesses and materials. Figure 3 shows SPR joints in the Body in White of a car.

.

SPR

Figure 3: SPR joints in the BIW of a car (Blackmore, 2007)

1.5 Summary of the introductory chapter

The chapter discusses briefly, the phenomenon of fatigue and the general methodologies of fatigue estimation. The stress life methodology was looked in some conceptual depth as a preferred methodology for spot joints. It also briefly discusses the new joining technique preferred in aluminium car body applications - self piercing rivets.

2. SPR Fatigue Failure Mechanisms

2.1 Aim of the chapter

The aim of this chapter is to study and analyse the SPR fatigue failure mechanisms observed in laboratory tests. Observations from these tests can be used to define an approximate generic SPR fatigue failure mechanism. Such an understanding of SPR fatigue failure mechanism can then be used to aid the creation of an SPR fatigue estimation model.

The identification of the forces that cause fatigue failure of SPR in car bodies may be attempted by studying the fatigue failure mechanisms observed during laboratory tests of SPR. In the following sections, 2 studies - Peter Blackmore study, and the Coventry University study, will be looked into.

2.2 Peter Blackmore study

Peter Blackmore (2007) has provided a near exhaustive insight into fatigue failure modes and damage mechanisms based on analysis of joints tested in laboratory.

The major failure modes identified for SPR fatigue failure were as follows:

1) Eyebrow crack failure mode
2) Stress concentration failure mode
3) Button failure mode
4) Rivet failure mode

2.2.1. Eyebrow crack failure mode

This is the most common failure mode observed in laboratory test conditions. Failure initiation is usually not visible on the outside of the sample as it happens at the sheet-sheet

interface and the crack propagates inside out. There is fretting between the top and bottom sheets which creates a stress concentration and initiates failure. There is bending and axial load acting on the joint during fatigue test causing a failure across the width of the top sheet passing through the circumference of the rivet head. Figure 4, Figure 5 and Figure 6 show the eyebrow failures observed in this study.

Figure 4: Eyebrow crack (Blackmore, 2007)

Figure 5: Eyebrow crack (Blackmore, 2007)

Figure 6: Fretting damage and eyebrow crack (Blackmore, 2007)

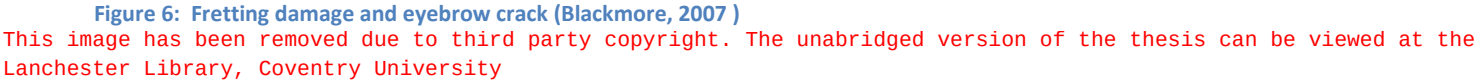

2.2.2. Stress concentration failure mode

This failure mode is due to the plastic deformation of the top sheet that takes place during the SPR joining process. The joining process causes a hole in the top sheet of the SPR joint which creates a stress concentration which serves as a location for failure initiation. The failure looks very similar to eyebrow failure; however the crack travels more around the circumference of the rivet head than an eyebrow failure as it propagates. Closer post test examination of the sample suggests that the cracks have originated diametrically opposite to each other at the hole produced on the top sheet during the joining process. There is very little to no evidence of fretting in this failure mode. Axial force can be considered as the dominant cause for this mechanism. Figure 7, Figure 8, Figure 9 show the stress concentration failures observed in the study.

Figure 7: Stress concentration failure (Blackmore, 2007)

Figure 8: Stress concentration failure (Blackmore, 2007)

Figure 9: Stress concentration failure (Blackmore, 2007)

2.2.3 SPR button Crack Failure Mode

Figure 10: Button failure (Blackmore, 2007)

Figure 11: Button failure (Blackmore, 2007)

This failure is initiated due to ductility exhaustion of the bottom sheet. During the SPR joining process the bottom sheet in some instances reaches its ductility limit during its plastic deformation. This limits its ability for further deformation during loading. Therefore the ductility exhaustion region serves as a crack initiation location. It is suggested that this failure does not have any effect on the mechanical performance of the joint as there is no load transfer taking place through this failure location i.e. the button in the joint configuration for shear and peel fatigue tests. This failure mode is mainly but not exclusively found in SPR with flat button. Figure 10, Figure 11, Figure 12 show the button failures observed in this study.

Figure 12: SPR button failure mode cross section (Blackmore, 2007 p12)

2.2.4. Rivet Failure mode

This is the failure of the rivet leg. In the unlikely event that the rivet suffers a static overload during the joining process, some damage may be accumulated in the rivet leg. This can serve

as a crack initiation location during cyclic loading. Figure 13, Figure 14 and Figure 15 show the rivet failures of this study.

Figure 13: Rivet Failure mode (Blackmore, 2007)

Figure 14: Rivet Failure mode (Blackmore, 2007)

Figure 15: Rivet Failure Mode (Blackmore, 2007)

The eyebrow failure mode is the most dominant failure mode observed. The dominant mechanism leading to initiation of crack is fretting between the top and bottom sheets.

2.3 Coventry University study

A series of tests at various load levels were done at Coventry University, to study the fatigue behaviour of SPR. The tests were led by Dr Paul Briskham with assistance from the author. The test specifications are as follows:

Test samples:

NG5754 SPR lap-shear specimens.

Top sheet thickness: 2 mm

Bottom sheet thickness: 3 mm

Rivet material and configuration: Specified by rivet manufacturers Henrob ltd.

Test preparation:

1. Load cell and LVDT need to be calibrated to the BS standard
2. Grips need to be aligned properly
3. Specimens need to be checked without too much bend (if so the proper adjustment needs to be added)
4. Proper machine tuning needs to be carried out

Test parameters:

1. Load control with proper compensation to ensure accuracy of the load (no bigger than +-5%).
2. Test frequency f=10Hz
3. Load ratio R=0.1
4. Load levels
    a. F_{max} = 8.0 KN
    b. F_{max} = 5.5 KN
    c. F_{max} = 3.0 KN
5. Failure criterion: 1 mm extension of the specimen

Test data recording:

The following data need to be recorded during the fatigue test in columns:

1. Number of cycles
2. Maximum displacement in mm (actuator)
3. Minimum displacement in mm (actuator)
4. Maximum load in N
5. Minimum load in N.

The data need to be recorded at following number of cycles:

a. F_{max} = 8.0 KN – every 500 cycles
b. F_{max} = 5.5 KN – every 1000 cycles
c. F_{max} = 3.0 KN – every 5000 cycles

Test procedures

1. Zero the load
2. Under displacement control, mount the specimen without overload.
3. Switch to load control
4. Apply zero load and zero the displacement
5. Set trip (load trip limits – 10% of Max/Min load, and the lower displacement, e.g. -0.3 mm)
6. Apply the maximum load for the fatigue test to the specimen, and apply zero load again when the displacement stabilised.
7. Start the fatigue test

8. Set the upper displacement limit by adding 1 mm to the maximum displacement achieved during the fatigue test (after 1000 cycles).
9. Run the test until upper displacement tripped.
10. Record the number of cycles for the failure.

The results of the tests are looked at in the following sections.

2.3.1 Tests with maximum load of 3 KN

Fatigue tests conducted at a maximum load level of 3 KN with an R ratio of 0.1 produced the eyebrow failure shown in Figure 16 at the end of 1.63 million, and the eyebrow failure shown in Figure 17 at the end of 1.54 million cycles.

Figure 16: Eyebrow failure at maximum load of 3 KN at 1.63 million cyles

The failures are similar to the circumferential failures found in the Peter Blackmore study mentioned in section 2.2.1. A study of the samples also indicates that the failure initiated at

the top sheet – bottom sheet interface, similar to the eyebrow failure mentioned previously in the chapter.

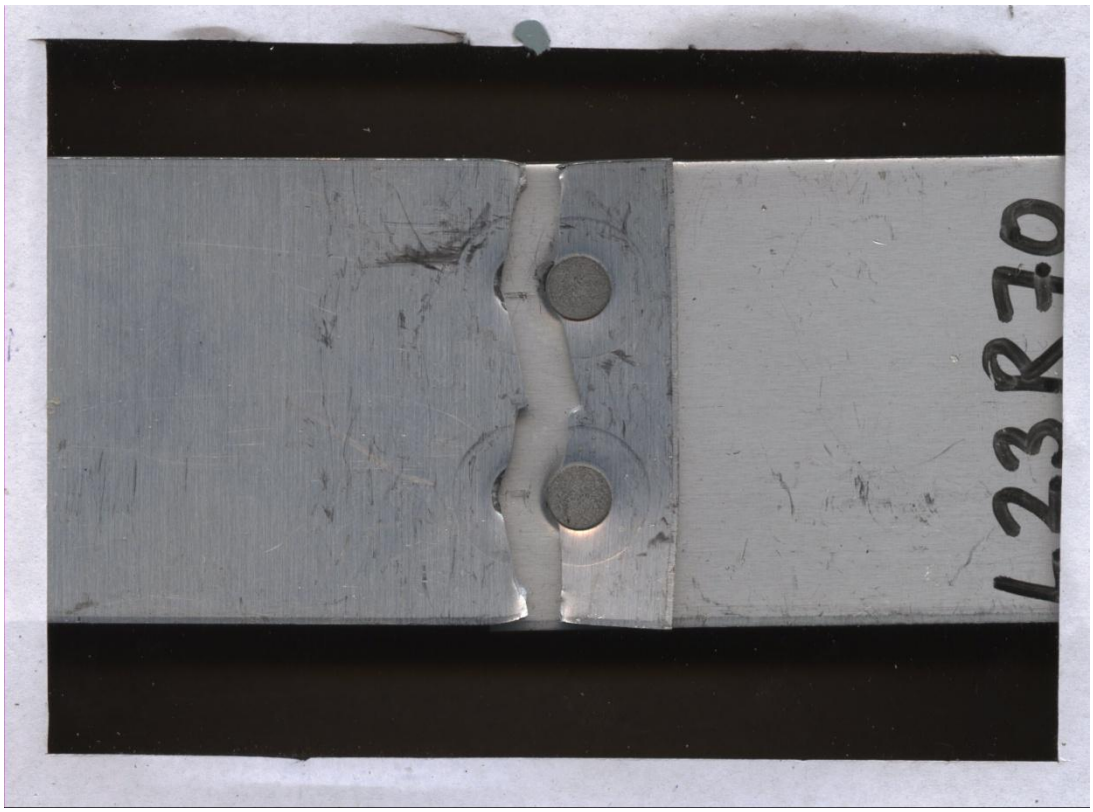

Figure 17: Eyebrow failure at maximum load of 3 KN at 1.54 million cycles

2.3.2 Tests with maximum load of 5.5 KN

A similar set of fatigue tests with a maximum load of 5.5 KN and an R ratio of 0.1 resulted in eyebrow failures as shown in Figure 18, Figure 19 and Figure 20 at approximately 0.13, 0.13 and 0.18 million cycles respectively.

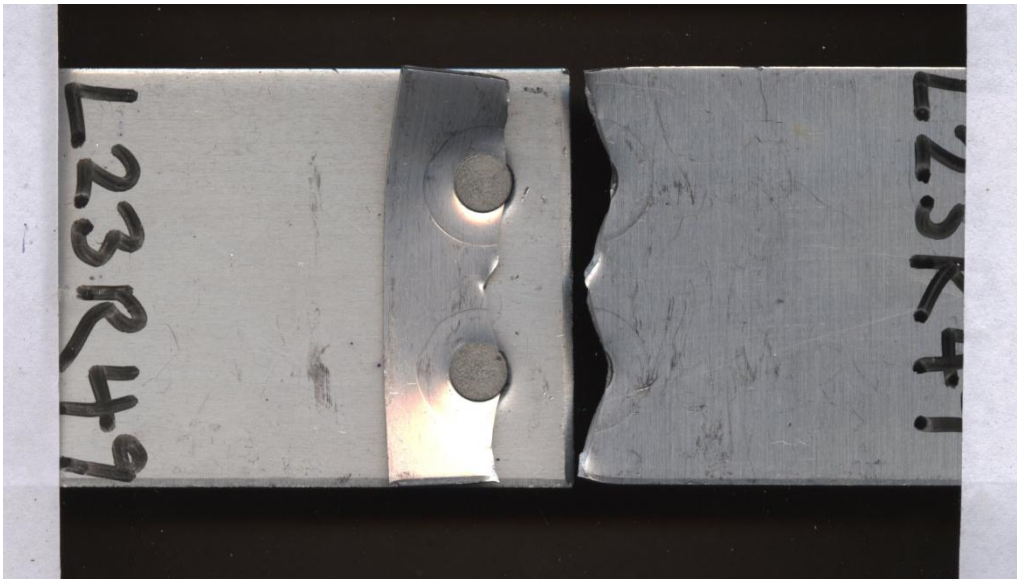

Figure 18: Eyebrow failure at maximum load of 5.5 KN at 0.13 million cycles

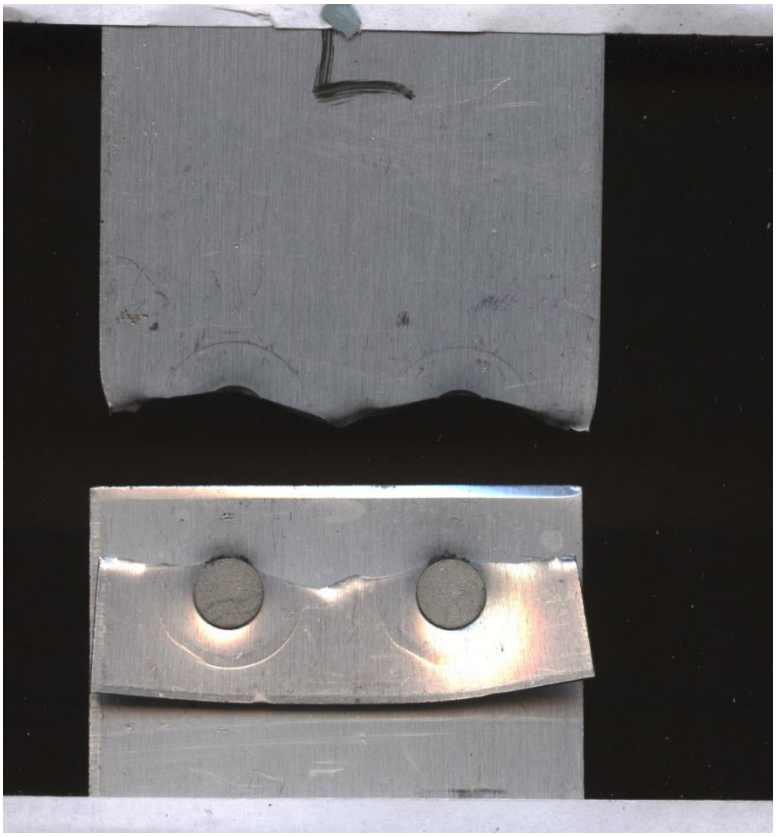

Figure 19: Eyebrow failure at a maximum load of 5.5 KN at 0.13 million cycles

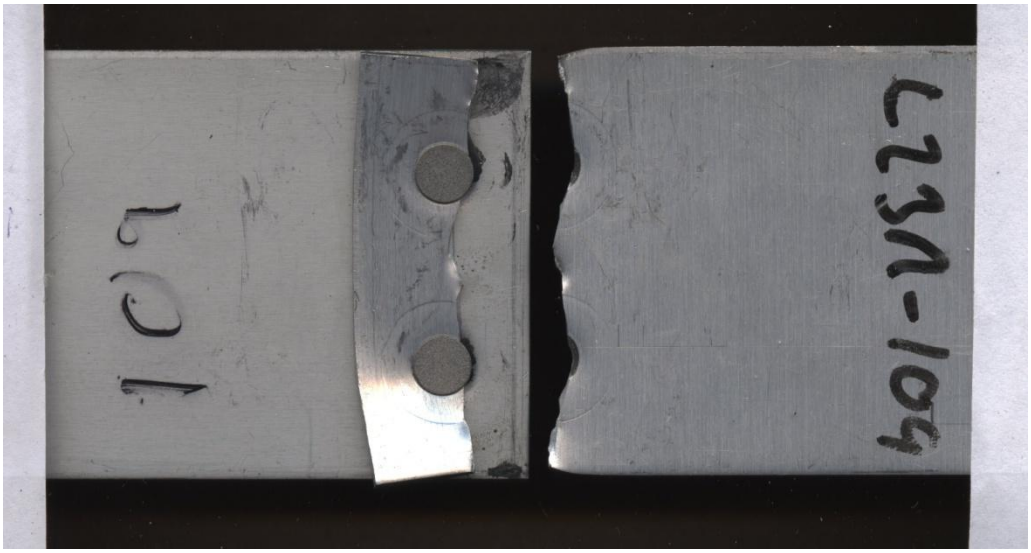

Figure 20: Eyebrow failure with 5.5 KN maximum load at 0.18 million cycles

All three tests done at a maximum load of 5.5 KN also show failure initiation at the sheet – sheet interface. The failure mechanism is similar to the ones mentioned in the previous section at a maximum load of 3KN and the failure mentioned in section 2.2.1

2.3.3 Tests with maximum load of 8 KN

Three tests with a maximum load of 8 KN and an R ratio of 0.1 were conducted. The samples shown in Figure 21, Figure 22, and Figure 23 had a fatigue life of 63000 cycles, 54000 cycles and 51,000 cycles respectively.

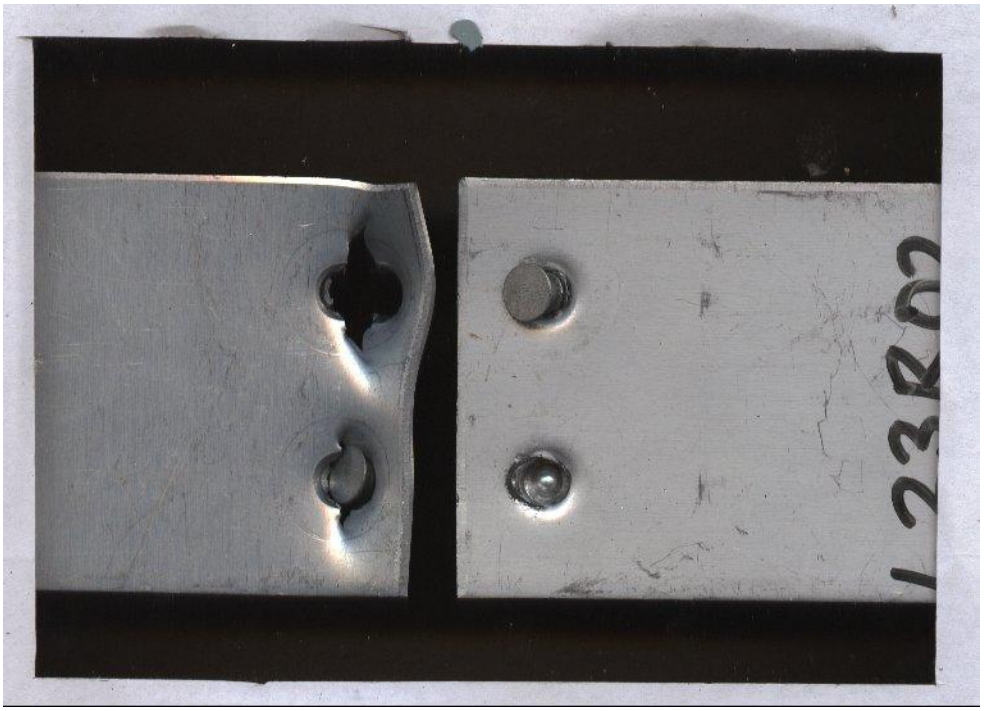

Figure 21: 3-9 failure at a maximum load 8 KN at 63000 cycles

Figure 22: 3-9 failure mode at maximum load 8KN and 54000 cycles

Figure 23: 3-9 failure at maximum load 8 KN at 51000 cycles

The failures with 8KN max load resemble the circumferential failure mode, or the stress concentration failure mode mentioned in section 3.1.2. They are also called the '3-9 failures'. Upon examination of the failed sample, it can be said that the failure has originated diametrically opposite to each other on the top sheet. There is no evidence of fretting between the sheets.

The force-life curve obtained by the fatigue tests mentioned above is shown in Figure 24.

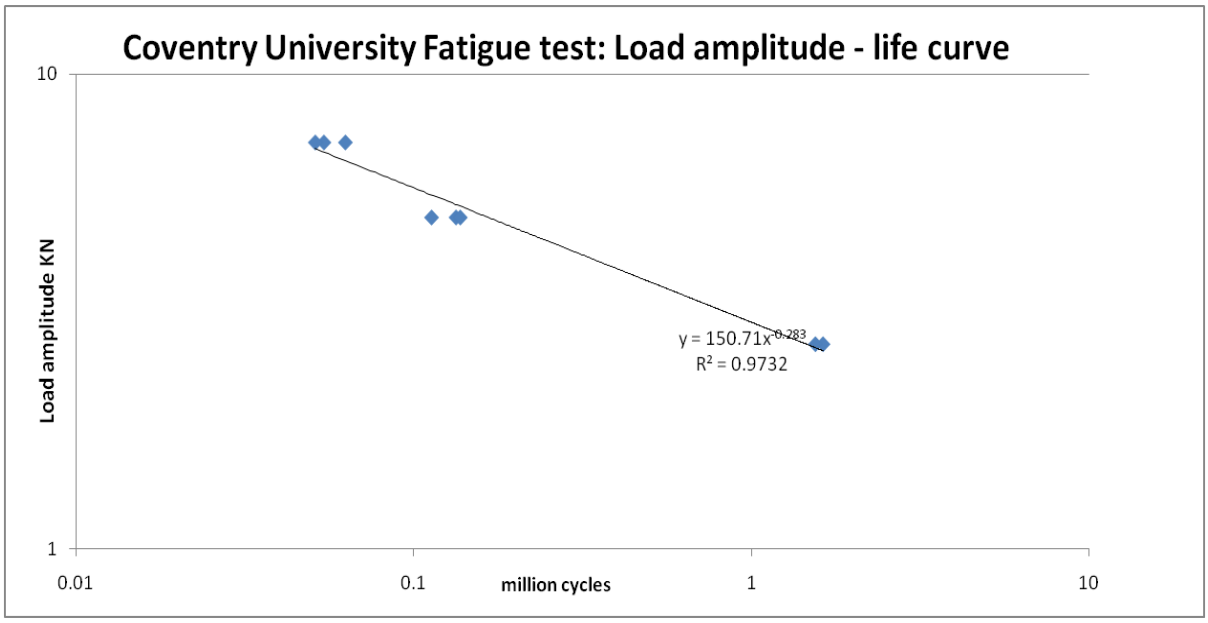

Figure 24: Coventry University SPR fatigue force-life curve

2.3.4 Key observations from the Coventry University Study

- As the load amplitude increases, the fatigue life decreases. 3KN max-load fatigue tests have the highest fatigue life, followed by the 5.5 KN and 8 KN tests respectively.

- Even though the observed fatigue lives are different based on the load amplitude, the 3 KN and 5.5 KN tests showed similar fatigue failure mechanisms. It may be noted that for automotive applications, failure initiation is the point of interest. Both 3 KN and 5 KN tests have the top sheet – bottom sheet interface as the failure initiation location.

- The 8 KN tests show a completely different failure mechanism, in that the failure initiation took place at the top sheet, diametrically opposite to each other. There is no evidence of fretting between the sheets in this failure mode.

2.4 Summary of the chapter

The key points to be noted from the chapter are as follows:

- The eyebrow failure mode, or the circumferential failure mode:

  According to the Blackmore study mentioned in section 3.3, the eyebrow failure alternatively called the circumferential failure is the major and the most significant SPR fatigue failure mechanism. The Coventry University study, also shows this failure mode as the chief failure mode, as it was observed in both the 3 KN maximum load and 5.5 KN maximum load tests.

- The top sheet – bottom sheet interface location of failure initiation:

  In the circumferential (eyebrow) failure mechanism, the failure initiation location is the interface between top and bottom sheet. This is noted by both the studies.

- Fretting:

  For the eyebrow failure mechanism, the failure initiation location in the samples show a black residue generally believed to be the evidence of the phenomenon called fretting. This is dealt with in detail in the next chapter. Being a mechanical joint, the SPR at microscopic level undergoes relative motion at the interface location of the sheets under load cycles. This relative motion between sheets initiates the eyebrow failure in SPR. Therefore, an effective fatigue estimation model for SPR must ideally take into account the effect of fretting.

- 3-9 failure, or the stress concentration failure:

The 8 KN maximum load fatigue tests conducted at Coventry University which produced a 3-9 failure, seems to resemble the stress concentration failure mentioned at section 3.3.2. The failure originated diametrically opposite to each other. There is no black residue found at the location during post test examination, suggesting that there is no evidence of the phenomenon fretting mentioned above.

3. Fretting Fatigue

3.1 Aim of the chapter

The objectives of this chapter are:

- To understand the phenomenon of fretting.
- To understand fretting fatigue.
- To understand fretting in SPR
- To deduce a fretting fatigue estimation methodology

3.2 Introduction

Fretting refers to small amplitude oscillatory movements between two surfaces in contact (Sum et al., 2005 p403). This interaction can eventually lead to failure through *fretting fatigue*. Fretting fatigue is a type of fatigue that can be produced when there are two bodies in contact and at least one of them is subjected to variable force (Muñoz et al., 2007 p2168). It is a phenomenon which is believed to significantly reduce the fatigue life of components (Sum et al., 2005 p403). It can also be defined as:

- A process of cyclic material damage accrual resulting from stress induced micrometer scale relative movements at the interface between contacting bodies. (Iyer, 2001 p193)
- An accelerated surface damage occurring at the interface between contacting materials subjected to oscillatory movements. (Elkholy, 1996 p265)

A study of fretting in self piercing rivet aluminium sheet was done by Chen et al (2003) with key findings as follows:

The types of fretting can be divided into:

1. Two body fretting
2. Three body fretting

3.3 Two body fretting

This is a phenomenon where the fretting takes place due to relative motion between two metal bodies. The occurrence of this phenomenon also corresponds to the stage in the fretting process that results in micro-crack initiation. The report stated that there were multiple cracks observed using the scanning electron microscope (SEM) study initiating at angles 15®-35® from the surface of the alloy. Figure 25 is a typical SEM image of the surface that underwent two body fretting.

Figure 25: SPR 2 body fretting SEM image (Chen et al., 2003 p1467)

3.4 Three body fretting

This is the fretting phenomenon that succeeds the two body fretting behaviour and involves the interaction between the two moving bodies and fretting debris created between them. It is suggested in the report that three body fretting causes abrasive damage to the surface where fretting takes place in addition to the kind of damages that are known to take place in two body fretting. Figure 26 is the SEM image of the two body and three body fretting zones in a sample.

Figure 26: SEM image of boundary between 2 body and 3 body fretting zones in SPR (Chen et al., 2003 p1466)

3.5 SPR fretting locations

According to the study mentioned above there are two major fretting locations in an SPR:

1. Fretting at the top sheet- bottom sheet interface
2. Fretting at the interface between rivet and joined sheet

Figure 27: SPR interfaces and fretting locations (Chen et al., 2003 p1464)

Figure 27 shows the interfaces of the SPR joint and location prone to fretting.

3.5.1 Fretting at the sheet - sheet interface

A study of SPR failure mechanisms by Peter Blackmore (2007) mentioned in one of the previous sections of the thesis also indentifies the interface between top sheet and bottom sheet as a location where fretting damage takes place. Figure 28 shows the fretting damage shown at the sheet – sheet interface during post test examination of a sheet stack joint by SPR. Figure 29 shows the suggested failure initiation location created at the top sheet-bottom sheet interface due to fretting according to the study conducted by Chen et al (2003 p1463).

Figure 28: SPR sheet-sheet interface fretting damage (Chen et al., 2003 p1463)

Crack initiation location

Figure 29: SEM image of fretting crack initiation (Blackmore, 2007 p8)

3.5.2. Fretting at the rivet – sheet interface

It was suggested that there was some evidence of circumferential fretting scars on the rivet due to movement between the rivet and the joined sheet. Figure 30 below shows the circumferential scar on the rivet.

Figure 30: fretting scar on rivet (Chen et al., 2003 p1465)

3.6 Fretting fatigue life estimation model

Navarro et al (2003) proposed a methodology to estimate total fatigue life in fretting fatigue. This methodology has been widely used for the development of fretting fatigue endurance curves and analysis of fretting fatigue lives of various structures. (Navarro and Domínguez, 2004), (Cadario and Alfredsson, 2005), (Muñoz et al., 2006), (Garcia and Grandt, 2007), (Muñoz et al., 2007), (Navarro et al., 2008), (Fadag et al., 2008) (Buciumeanu et al., 2008), (Santus and Taylor, 2008), (Vazquez et al., 2010). This methodology is developed similar to the Socie et al. (1979) model for estimation of total fatigue life of notched and cracked components. However, it has not been previously applied on fretting fatigue. (Navarro et al., 2003 p460)

According to this methodology, the entire fretting fatigue life can be divided into two stages:

1. Failure initiation
2. Crack propagation

Both the stages go through entirely different mechanisms and are dealt separately. Some cases go through the initiation mechanism more than the propagation, and some cases have a higher propagation life than failure initiation life. Therefore, for each case an appropriate mechanism can be chosen over the other. In situations where both initiation and propagation share significant chunks of the fretting fatigue life, a combination of both mechanisms are used (Navarro et al., 2003 p460). For car body applications with significant stiffness requirements for the structure, the desired fatigue life of the joints do not lie in the crack propagation region. The existence of a significant crack may compromise on the

stiffness of the structure. Therefore, primary interest is for estimation of fatigue life till failure initiation.

3.7 Estimation of cycles to failure initiation due to fretting

According to Navarro et al. (2003 p460-461) a hypothetical value called *crack growth rate due to failure initiation mechanism* can be calculated. It is calculated by estimating the numbers of cycles taken for failure along the path of the crack and then taking its derivative. The life along the path is calculated by considering the equivalent stress along the length of the crack and using the stress life curve for the material or component. This damage rate is believed to be reduced as the crack depth increases, and overtaken by classical crack propagation rate calculated through facture mechanics which is believed to increase as crack depth increases. A combination of these two crack growth rates are considered in components or applications where both crack initiation and propagation are considered vital in the life evaluation process.

The process is represented graphically as follows:

- Developing a stress-strain life curve for the material/component under consideration. A stress-strain life curve is a strain-life curve in which an equivalent stress is used to estimate the life when the strain remains relatively constant. Alternatively, it may also be called as a stress-life curve, where strain is used when the life of the sample is in the plastic regime. As mentioned in the introductory chapter, strain life methodology is preferred when the life of the sample is in the plastic regime, and stress life methodology is preferred when the life of the sample is in the plastic regime.

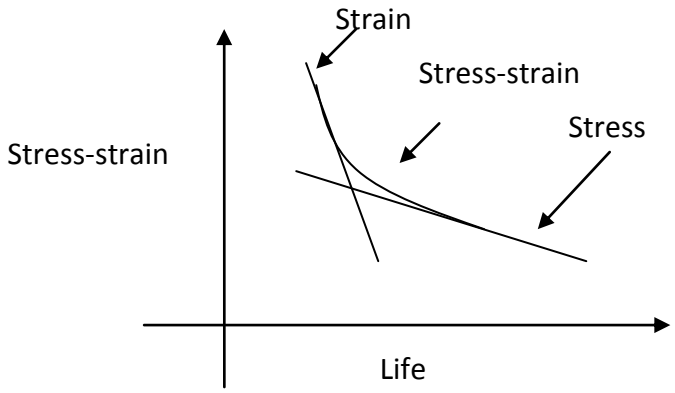

Figure 31: Stress-strain life curve

- Calculating the equivalent stress along the crack path is calculated using the stress life curve of the material/component.

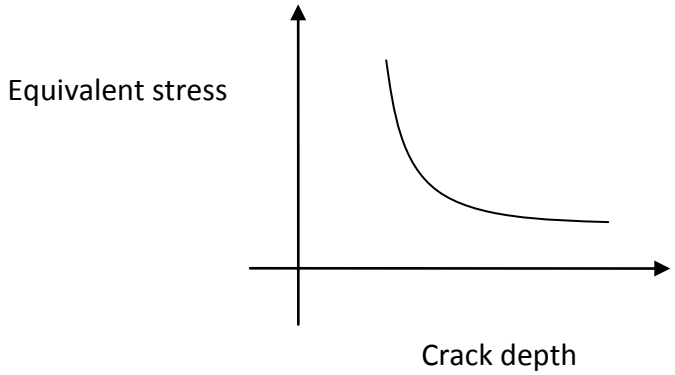

Figure 32: Equivalent stress - crack depth

- Combining the two curves above, assuming the y axis of both Figure 31 and Figure 32 to be the same, a relationship between cycles to failure and crack depth is achieved.

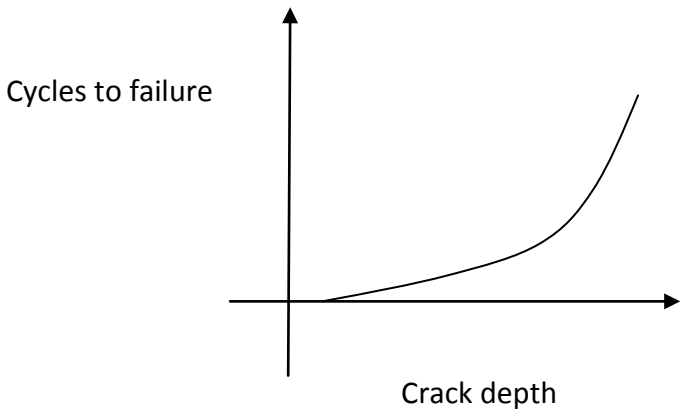

Figure 33: Cycles to failure - crack depth

- The derivative of the above gives a hypothetical *crack growth rate due to initiation*

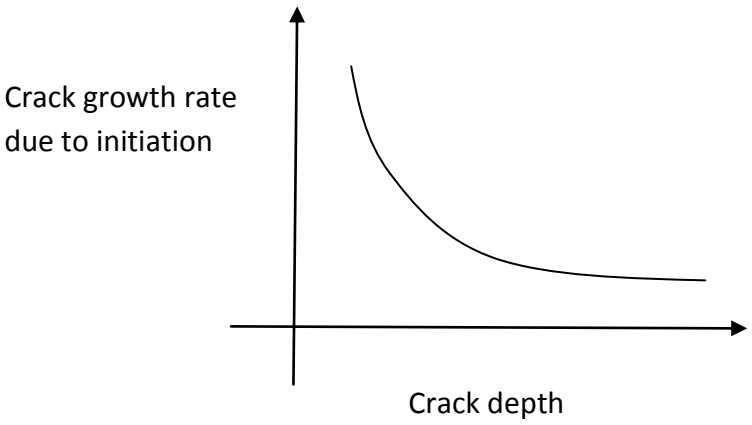

Figure 34: Crack growth rate due to initiation

3.8 The stress criteria for fretting fatigue failure initiation

A study was conducted in 2001 (Lykins et al.) to understand the fretting damage induced crack initiation of dove tail joints, and to develop an analytical model to estimate their fatigue life. The study suggested that the fretting crack initiation mechanism was governed

by maximum shear stress at critical plane (Lykins et al., 2001 p462). The validity of this finding was acknowledged by R. W. Neu (2008) of Georgia institute of technology in a study reviewing the advances in understanding the fretting fatigue behaviour of materials.

3.9 Summary of the chapter

In this chapter, the phenomenon of fretting fatigue was looked into. The fretting behaviour of SPR was also studied. Some existing guidelines for a fretting fatigue estimation methodology were pondered upon. Fretting fatigue estimation methodology may be distinctly divided into two stages:

- Failure initiation
- Crack propagation

Most importantly, shear stress at the critical plane is believed to govern the fretting failure initiation.

4. SPR Fatigue estimation models

4.1 Aim of the chapter

This chapter moves from a generic understanding of various fatigue estimation methodologies, SPR fatigue failure mechanisms and fretting, into specific models available in literature suited for the fatigue life estimation of SPR in car body. Two models are discussed:

1. The Dannbauer Model
2. The Rupp Model

The chapter aims to understand the rationale and logic behind each of these models in detail. The chapter also identifies the salient features of each model and tries to find commonalities between the two.

4.2 Introduction

The fatigue life estimation method of a car body structure consisting of SPR as the primary joining technique has the fatigue life estimation of the SPR themselves as its main constituent. To help automotive design engineers at the early stages of design and development to work towards a robust car body, there arises the need for a computer aided fatigue life estimation model for SPR joints. The need for a Finite Element post processing based fatigue estimation model is paramount, due to the large number of spot joints in a car body. Any inefficiency or lack of total confidence in the estimation model may inadvertently lead to the car body being over-engineered by the design engineers to avoid a failure.

4.3 Dannbauer et al. model

This fatigue estimation model for SPR have been developed analogous to pre existing working models used effectively for spot welds (Dannbauer et al., 2003p1). But since the fatigue properties of SPR are enormously different and more complicated to that of spot welds, significant modifications have had to be made for the model to be suitable (Dannbauer et al., 2003 p4). The model makes use of the linear Finite Element structural stresses and component stress life curves. The point joints are modelled through the following steps:

1. Location of the spot joints and the connecting sheets are identified.
2. A local mesh refinement is made around the location of the joint.
3. The connection is made using beam, rod or rigid elements.

The first two steps are automatically done by the SPOT pre-processor of FEMFAT fatigue software. The pre-processor can do the above steps in two different ways:

1. Mesh dependent method

In the case of mesh dependent method, locations of spot joints are specified by the user in the FE structure. The nodes that represent position of joints are marked off using colour or displacement coordinate system. A mesh refinement is then made around the point joint locations.

2. Mesh independent method

In the case of mesh independent method, the position of spot joints and connecting sheets are specified by CAD data. Then around the spot joints a mesh refinement is made similar to the one made in the mesh dependent method.

The modelling of SPR joints are performed using two concentric shell element rows around the centre spot joint node. The nodes of the inner row are located on a circle with the same diameter as the rivet shaft. The nodes on the outer row are located on a circle with same diameter as the rivet head. The sheets are connected using beam element with a pipe cross section. The outer diameter of the beam element is the same as the rivet shaft and the wall thickness of the beams the same as wall thickness of rivet shaft. To maintain correct stiffness of the SPR it is suggested that young's modulus of the elements in the inner row be 40 times the young's modulus of the basic material and the young's modulus of the elements in the outer row be 6 times that of the basic material. The young's modulus of the connecting beam is a function of the rivet diameter and sheet thickness.

Figure 35: Pre-processing of spot joints (Helmut et al., 2004 p5)

Figure 36: Model of SPR joint (Helmut et al., 2004 p6)

The influence of the rivet diameter and the sheet thickness on the young's modulus of the beam element is represented by the following formula:

$$E\ beam = C.t^{p1}.\left(\frac{D\ rivet}{5.3}\right)^{p2}$$

Equation 1: Young's modulus of the beam element

Where,

E beam = Young's modulus of the beam element

C = Material constant

t = Equivalent sheet thickness

D rivet = Rivet shaft diameter

p1 and p2 = Material exponents

The material constant C has a value of 5 GPa for Aluminium. The equivalent sheet thickness is half the sum of top and bottom sheet thicknesses.

For fatigue estimation the von mises stresses at the outer shell row elements and nodes are used. It may be possible later on to use other stresses like radial and tangential stresses for fatigue estimation. Component Stress life (SN) curves are used to calculate the estimated life. The influence of variation in parameters like sheet thicknesses, rivet dimensions and loading are stored in the form of modifications to SN curves in the data base i.e. a different SN curve for each variation. The effect these parameters are observed to be non-negligible in some cases.

The effects of variations are captured as follows:

1. Variation in loading direction :

Influence of different loading types has been captured in the form of SN curves from cross tension coupon tests, shear coupon tests and the combinations thereof. Considering pure shear as 0® load and pure cross tension as 90® load, SN curves have been specified for a step of 15®.

2. Variation in sheet thicknesses:

SN curves for different sheet combination are captured and stored in database for appropriate use during the fatigue estimation process. It has been observed that for the same material, rivet diameter and loading, the parameters of the SN curves i.e. slope, fatigue limit etc. varied significantly with change in sheet thickness.

3. Different rivet diameters:

The variation in fatigue life based on difference in rivet diameter is also captured using a variation of SN curve parameters for each rivet diameter.

These modifications can be expressed in the following equations:

$$\sigma_D = \sigma_{D.ref}.t^{p3}$$

Equation 2: SN curve Fatigue limit (Helmut et al., 2004 p7)

$$k = k_{ref}.t^{p3}$$

Equation 3: SN curve slope (Helmut et al., 2004 p7)

$$N_D = N_{Dref}.t^{p5}$$

Equation 4: SN curve cycle limit (Helmut et al., 2004 p7)

Nomenclature of equations 2, 3 and 4:

σ_D = fatigue limit of the SN curve of the current spot joint with equivalent sheet thickness t

σ_{Dref}= fatigue limit of the SN curve of the spot joint with 1 mm equivalent sheet thickness used as reference

t = equivalent sheet thickness

k = slope of the SN curve of the current spot joint

k_{ref} = slope of SN curve with 1 mm equivalent sheet thickness used as reference.

N_D = cycle limit of the SN curve of the current spot joint

N_{Dref} = cycle limit of the SN curve of the spot joint with 1 mm equivalent thickness used as reference

4.3.1 Coupon configurations used for fatigue tests in the model

Several sheet thickness combinations ranging from 0.7 mm to 2.77 mm were used. The rivet diameters used were 3mm and 5 mm. The specimen types used for the tests were:

- Lap shear configuration (Figure 37)
- T peel configuration (Figure 38)
- H specimens (Figure 39)

Figure 37: Lap shear test specimen

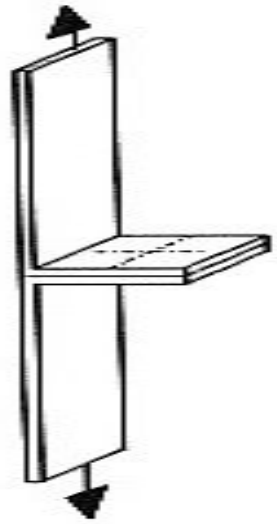

Figure 38: T peel test specimen

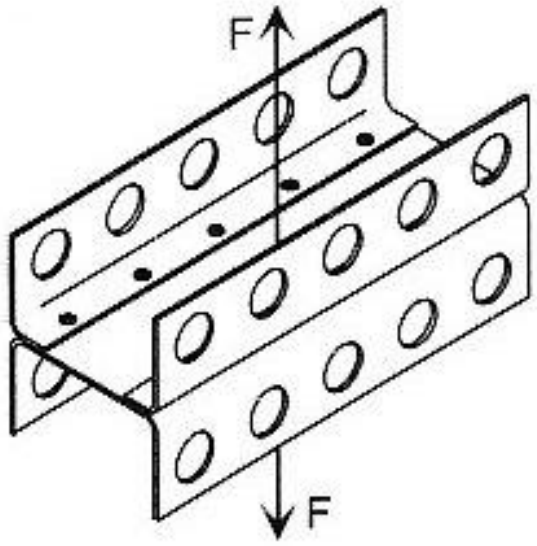

Figure 39: H specimen

4.3.2 Key points of the model

- The model has been developed analogous to the pre existing spot weld fatigue estimation model
- It has been acknowledged that even though the estimation model has been developed from pre-existing spot weld model, the fatigue properties of SPR vary hugely from that of spot welds and are more complicated. The two clear differentiating factors in the model between the spot welds and SPR being:
    - The modifications in the modelling of the SPR joint
    - The modifications in the stress life curve
- It has been observed during the course of fatigue testing for the model that the fatigue life of SPR varies significantly with parameters like sheet thickness, rivet diameter, specimen type, load etc (Helmut et al., 2004 p6). The most important of these is the influence of sheet thickness.
- An attempt has been made to capture the influence of various parameters using modifications of SN curves.
- The rationale behind the configuration of the test specimens that were used have not been adequately addressed or explained.
- The rationale behind some of the heavy improvisations made in terms of adjusting the young's modulus has not been clearly explained.
- The model relies heavily on the analysis test data.
- No attempt has been made to understand the physics of the fatigue failure of SPR joints and incorporate it into the estimation model.

- Variations in loading have been accounted for entirely by modification to SN curves, based on test data of various sample configurations.

- An intrinsic and logical limitation may arise due to the fact that the model has been developed analogous to a spot weld fatigue estimation model. Spot welds and SPR differ hugely in fatigue behaviour as mentioned earlier. The modifications that would suit the model for use in SPR have not been critically argued.

4.4 Rupp Spot weld Model

One of the widely accepted spot weld models analogous to or in reference to which other spot joint fatigue estimation models have been developed is the *Rupp et al* model (Helmut et al., 2004 p4), (Zhang and Taylor, 2001 p1013), (Kang and Barkey, 1999 p765), (Kang, 2007 p837), (Donders et al., 2006 p676), (Fermér et al., 1999 p2), (Heyes and Fermer, 1996). The aspects of the model which have been used to develop a model suited to fatigue life estimation of SPR and other spot joints are as follows:

1. Identifying the key forces and moments acting through the joint or the locations in close proximity to the joint that contributes towards fatigue failure.
2. Conversion of the forces and moments that pass through the joint into its corresponding structural stresses.
3. Estimating the life of the joint using the appropriate stress life curve developed through fatigue tests.

Understanding the failure mechanism of the joints is linked with identifying the key forces and moments that cause fatigue failure, and the conversion of these into their corresponding structural stresses. A spot weld joint can fail due to fatigue through: (Rupp et al., 1995 p6)

1) The sheet metal
2) The weld nugget

The structural stress causing failure due to forces and moments in the sheet metal is calculated as follows: (Rupp et al., 1995 p7)

$$\sigma_{shear} = \frac{F_{shear}}{\pi d s}$$

Equation 5 : Structural stress in the sheet due to resultant shear force in the point joint

$$\sigma_{axial} = \frac{1.744\, F_{axial}}{s^2}$$

Equation 6 : Structural stress in the sheet due to axial force through the point joint

$$\sigma_{bending} = \frac{1.872\, M}{d s^2}$$

Equation 7 : Structural stress in the sheet due to bending moment at the point joint

The structural stress causing failure due to forces and moments through the joint nugget is calculated as follows: (Rupp et al., 1995 p7)

$$\sigma_{shear} = \frac{16\, F_{shear}}{3\pi d^2}$$

Equation 8 : structural stress at the point joint due to the resultant shear force

$$\sigma_{axial} = \frac{4\,F_{axial}}{\pi d^2}$$

Equation 9 : Structural stress in the point joint due to axial force

$$\sigma_{bending} = \frac{32M}{\pi d^3}$$

Equation 10 : Structural Stress at the point joint due to bending moment

Nomenclature of equations 5, 6, 7, 8, 9 and 10:

σ_{shear}= Structural stress due to the resultant of the shear forces at the point joint

σ_{axial}= Structural stress due to axial force at the point joint

$\sigma_{bending}$= Structural stress due to bending moment at the point joint

F_{shear}= Resultant shear force on the point joint

$F_{axial=}$ Axial force through the point joint

S= Equivalent sheet thickness

M= Bending moment at the point joint

d= Spot joint diameter

The various forces acting through the point joint are shown in Fig6. The forces and moments that cause fatigue damage are assumed as follows:

1) Axial force acting through the point joint: F_z
2) Shear force acting on the joint*:* F_x, F_y
3) Bending moments: M_x , M_y, M_z

Figure 40: Forces and moments acting on an analytical spot weld nugget (Helmut et al., 2004 p4)

4.4.1 Key Points

- The methodology adopted by Rupp et al model of fatigue estimation has been widely used to develop other models for fatigue estimation for spot joints.
- The equations converting forces and moments through the spot joints into its corresponding stress have been developed in relation to the spot weld failure mechanisms.
- The need for theoretical understanding of the failure has been emphasised as it is suggested that the fatigue behaviour of the test specimens in laboratory might not be representative of the fatigue behaviour of the joints in the car body.
- Specific reasons behind the choice of the test specimens that were used to generate data, were not given.
- The model takes into the account the failure mechanism specific to the joint type and uses a combination of test data and an attempted understanding of the physics

of the fatigue behaviour for fatigue life estimation. However, the joint type in consideration is spot welds and not SPR. Therefore, this model though ideal for spot welds, has its intrinsic limitations when improvised for use in SPR fatigue life estimations.

4.4.2 Test Specimens used in the model

The test specimens used in the model are:

- Hat profile

Figure 41: Hat profile test specimens for spot weld tests (Rupp et al., 1995 p8)

- T beam

Figure 42: T beam specimens (Rupp et al., 1995 p8)

- Single and double spot specimens

Figure 43: Double spot specimen (Rupp et al., 1995 p8)

- Load carrying beam

Figure 44: LC beam (Rupp et al., 1995 p8)

4.5 Summary

This chapter deals in detail with the models available for the fatigue life estimation of SPR in car body. It highlights its key features and some of its common limitations. The major points that may be noted from the chapter are as follows:

- The major intrinsic limitation that these two models have arises due to the fact that both these models at their core tend to deal with the fatigue properties of spot welds. Spot welds differ enormously and fundamentally from SPR.

- Rupp model has tended to deal with the physics of failure more than the Dannbauer model. The Dannbauer model has relied very heavily on laboratory data.

- Choice of test specimens for the lab tests have not been explained

5. Major gaps in existing SPR fatigue estimation models

The following sections will attempt to highlight some of the limitations of the Dannbauer model and the Rupp model.

5.1 A Common limitation in the rationale

Both the fatigue estimation models discussed have as a basis, the fatigue behaviour of spot welds, while it is a unanimously accepted and documented fact that the fatigue behaviour of spot welds and SPR differ hugely. While Rupp model was designed specifically for fatigue life estimation of spot welds, Dannbauer model has been developed analogous to it. This rationale constitutes the source of a major flaw in terms of getting appropriate estimations. Basing estimation on the behaviour of a joint whose fatigue life is significantly lower than that of SPR can lead to significant over-engineering.

5.2 The Dannbauer model

The Dannbauer model has been significantly changed to suit SPR fatigue estimation. The adjustments made include:

1. Adjustments in how SPR may be modelled in FE by design engineers:

These adjustments include:

- Changes in meshes and use of elements
- Changes in the young's modulus of the elements concerned

Both these adjustments have not been explained with adequate rigour, as to how they would attribute to representing SPR behaviour.

2. Adjustment to Stress-life curves.

These adjustments cater to the following:

- Difference in fatigue life of SPR from that of spot welds

- Difference in sheet thicknesses
- Difference in loading angle

These adjustments account for a series of laboratory tests for all possible scenarios with fatigue life estimation of SPR, which gives rise to two major disadvantages:

a. With the need for a large amount test data, Repeatability & Reproducibility becomes a major issue. Therefore, significant resources need to be used in developing such a model to keep the errors and variations to a minimum.

b. Since there is no understanding of the physics of failure, improvisations cannot be made to accommodate any situation different from the laboratory test conditions. As soon as the car body would move on to conditions or load patterns different from the lab settings, the test data and hence the entire model would inch towards being not suitable, since the model relies completely on laboratory data. This could directly lead to over-engineering.

5.3 The Rupp spot weld model

This model has been designed for the fatigue estimation of spot welds. However, it has been used widely as a model for generic spot joints as mentioned previously. Dannbauer model has been developed analogous to it. It is a numerical model as highlighted in the previous chapter, which attempts to capture the physics of the fatigue failure through equations. Its fundamental limitation can be explained as follows: The stress equations derived in the model, calculate the stresses at the critical locations of a spot weld, for use in the stress life

methodology of fatigue estimation. Since the fatigue behaviour of SPR and spot welds differ hugely, the Rupp model cannot be used as it is to estimate SPR fatigue life.

5.4 Major Gap

The major gap in models available for fatigue estimation of SPR in car body can be expressed concisely as follows:

> There does not exist in literature, a numerical model for the fatigue estimation of SPR in car body structure, which is based on the observed fatigue failure mechanisms of SPR. Fretting, is believed to be a factor in the failure initiation of the dominant eyebrow failure mode of SPR. There is no model in literature, which attempts to capture the effect of fretting in the failure initiation of SPR for car body applications.

6. Development of a new Model

6.1 Aim of the chapter

The aim of the chapter to try and bridge the gap mentioned in section 5.4 of chapter 5, in light of knowledge of SPR fatigue failure mechanisms, mentioned in chapter 2. The chapter presents a new model for the fatigue life estimation of SPR in car body applications.

6.2 Introduction

There are 6 key points or pretexts to be remembered for the development of this model. They are:

1. Stress life methodology:

   It may be remembered as previously mentioned in the thesis, that stress life methodology is the preferred methodology for fatigue life estimation, when the desired life of the joint lies within the elastic regime. In aluminium car body applications, due to stringent requirements for a stiff body, a joint already under crack may be deemed as a failed joint. Therefore, the desired life of SPR may be considered to be within the elastic regime for this case. Thus, stress life methodology may be considered the preferred methodology in this case.

2. Lap shear loading:

   The spot joints in a car body are generally believed to be designed to endure shear load. The tests mentioned in chapter 2, for the study of SPR fatigue behaviour were conducted on lap shear specimens. Therefore, the fatigue behaviour of SPR under the lap shear configuration (Figure 46) may be assumed to be the most appropriate for developing a numerical model for SPR fatigue behaviour.

3. Fretting fatigue crack initiation criterion:

As mentioned in section 3.6 of chapter 3, the fretting fatigue crack initiation criterion is shear stress at critical plane. Therefore, at the top sheet – bottom sheet interface fretting location, as mentioned in section 3.5.1 of chapter 3, and the eyebrow failure crack initiation (due to fretting between sheet-sheet interface) location as mentioned in section 2.2.1, section 2.3.1, and section 2.3.2 of chapter 2 , the shear stress at the critical interface may be assumed as the fretting crack initiation factor.

4. Failure initiation:

As mentioned previously in the thesis, the car body has durability and stiffness requirements. Therefore, a joint significantly into a crack propagation phase, may be assumed as a failed joint. Therefore, a point hypothetically and approximately close to failure initiation in fatigue life, is what the estimation model must attempt to find.

5. Failure modes:

The eyebrow failure mode mentioned previously in the thesis is the dominant failure mode, and is affected by fretting fatigue. However, the 3-9 failure mode discussed in 2.3.3 of chapter 2, which is arguably the same as the stress concentration failure mode discussed in section 2.2.2 of chapter 2, is another valid failure mechanism for lap shear SPR specimens observed at higher loads as mentioned in section 2.3.4 of chapter 2. Therefore, the two SPR fatigue failure mechanisms that may be incorporated into the estimation model are:

- Eyebrow failure

- 3-9 failure

6. Sheet stack failure:

As noted in chapter 2, the majority of failures in Aluminium SPR samples take place at the sheet stack. It may be noted that it is not the rivet that fails in most cases, but the sheet that the rivet joins. Due to the geometry of SPR joints as shown in Figure 45, the load transfer location and the failure initiation location may be assumed to be at the sheet-sheet interface in the direction of the applied load, for a lap shear specimen. Therefore, the cross-section XX' (Figure 45) shown below becomes a plane of interest. It may be assumed that this cross section of sheet stack undergoes failure initiation at the interface location, aided by the phenomenon of fretting. Therefore, as mentioned in the above point, shear stress at the interface location in the XX' cross sectional plane, may be assumed as the fretting crack initiation factor. In simple terms, it may be assumed that:

The sheets stack cross-sectional plane (Figure 46) fails at the interface location due to shear stress at the interface, for an eyebrow failure in a lap shear specimen.

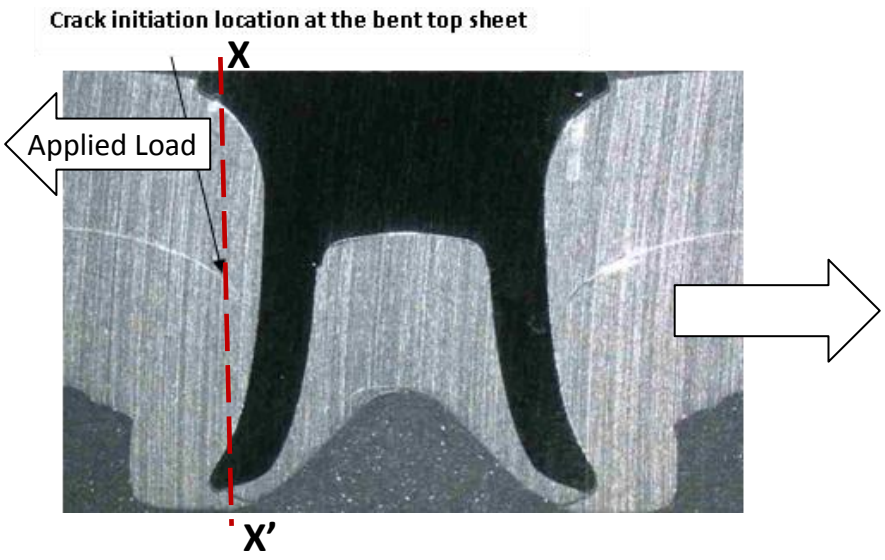

Figure 45: Major crack initiation location in SPR under lap shear loading

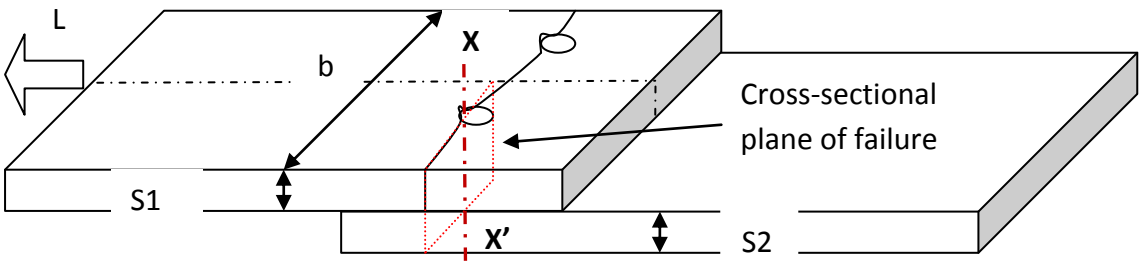

Figure 46: Eyebrow top sheet failure under lap shear loading

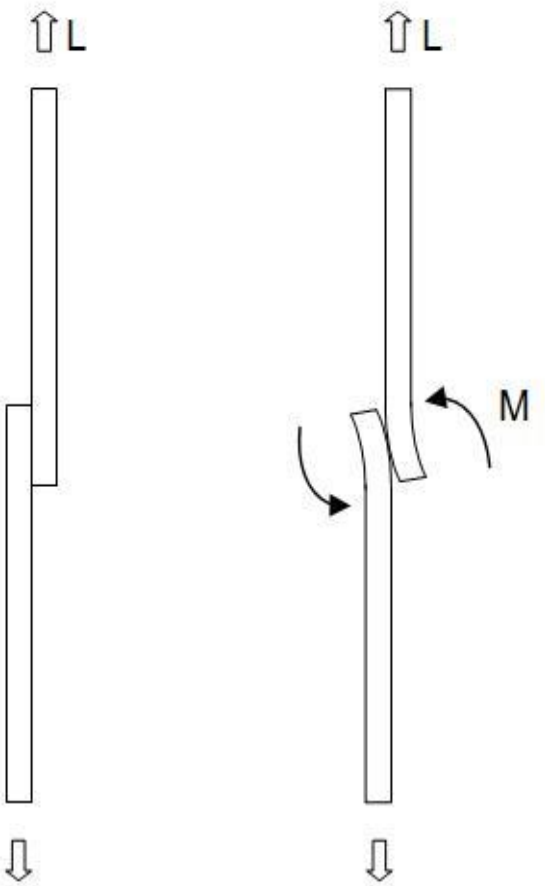

Figure 47: Bending induced during lap shear test

6.3 Derivation of stress equation for eyebrow failure mode

As shown in Figure 47, the lap shear specimen under load undergoes bending. Therefore, the cross sectional plane of failure, shown in Figure 46 undergoes bending.

Equation 11 is the standard formula for calculation of shear stress due to bending across the cross section of a rectangular cross sectional beam (Figure 48: Rectangular beam section). This formula can be adapted to calculate the shear stress at the interface location in the critical plane shown in Figure 46. It may be noted again, that shear stress is also considered the fretting failure initiation criteria. Thus, by using and adaptation of Equation 11 fatigue failure may be expressed as a combination of bending and fretting.

For a rectangular beam:

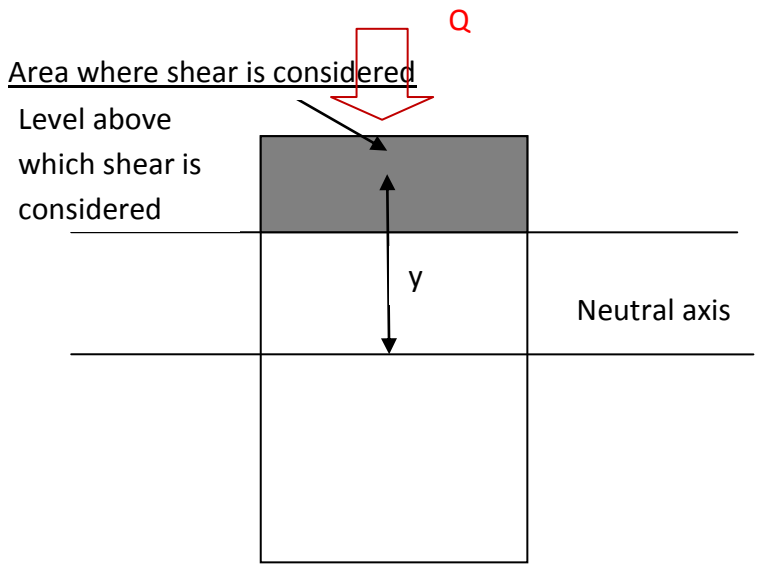

Figure 48: Rectangular beam section

$$\text{Shear stress } \tau = \frac{QAy}{Ib}$$

Equation 11: Shear stress due to bending

Where,

Q = The bending force that induces shear

A= Area of the section where the shear is considered

y = Distance from the neutral axis at the centre of the section to the centroid of the area A

I= Area moment of area of the whole section

b = width of the section at the level where shear stress is to be considered

<u>Considering the following assumptions:</u>

1) The flow of shear stress due to bending through the critical cross sectional plane varies approximately like shown in Figure 49. It implies maximum shear stress at the middle of the joint which also the interface and lower stresses towards the ends.

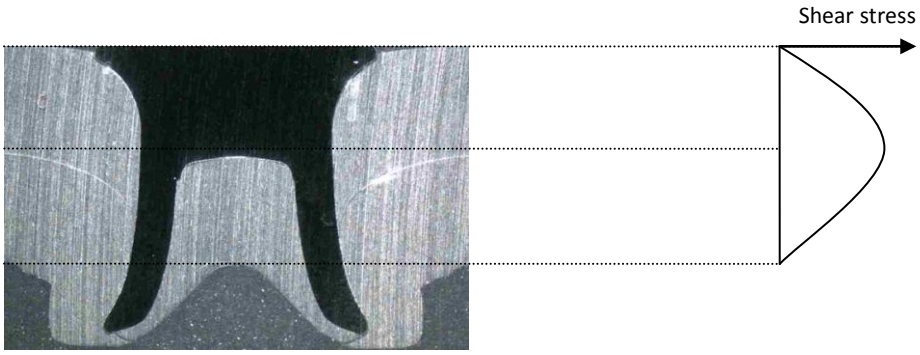

Figure 49: Approximation of shear stress through the length of the joint

2) It is the section *above* the middle axis that tends to shear off, based on the observation that the failure after initiating in the interface fails the top sheet.
3) The button (the bottom sheet protrusion due to the die) has no role to play in the load transfer.

Considering the critical plane of failure (Figure 50) i.e. the load withstood by one SPR (based on the symmetry of the two rivets in the Lap shear coupon (Figure 46), the equation for shear stress due to bending at the failure initiation location can be developed as follows:

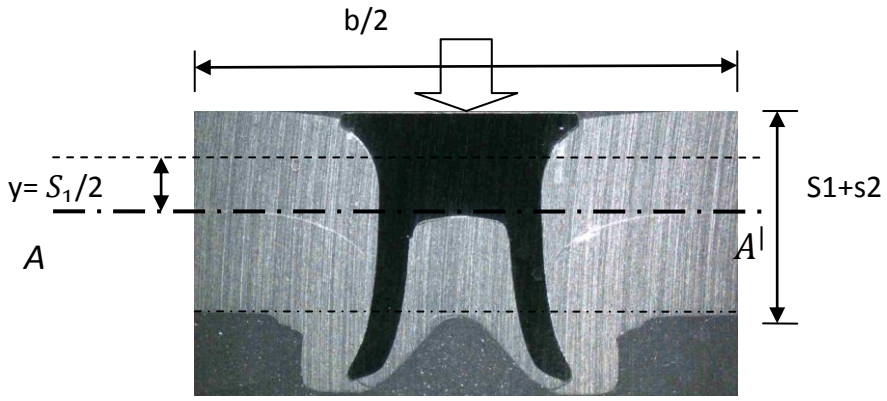

Figure 50: Shear stress at the sheet-sheet interface due to bending

Deriving Shear stress at level A-$A^{|}$ due to bending:

The variables of Equation 11 can be replaced as follows:

Q= Magnitude of the induced bending moment M. (Figure 47)

A= Cross sectional area of the top sheet where shear is considered: $\frac{b.S_1}{2}$ (Figure 50)

y= Distance from the interface to the centroid of A: $\frac{S_1}{2}$ (Figure 50)

I= bending moment of area of the whole section: $\left[\frac{b}{2} . (S_1 + S_2)^3\right]/12$ (Figure 50)

b= Width of the section at the level where shear is to be calculated: $\frac{b}{2}$ (Figure 50)

Therefore, by replacing the variables in Equation 11 by the values mentioned above, shear stress at level $AA^{|}$ due to bending, or the shear stress at sheet-sheet interface due to bending induced in the joint as a result of an applied load can be expressed as:

$$\tau = \frac{D_{f1.}12\ .M.{S_1}^2}{b.(S_1+S_2)^3}$$

Equation 12: Conversion of bending moment to stress (proposed model)

Where, D_{f1} is a Deformation factor, as the extent of deformation of the sheets based on the rivet dimensions, may be assumed to have an effect on the breaking down of the applied load into various components, M is the bending moment induced as a result of the applied load.

D_{f1} factors in the distance element by which the applied force gets converted to a bending moment. It may be assumed as proportional to the inverse of the distance that converts the force on the joint to a bending moment. Therefore, in the Equation 12 it allows M to be the magnitude of the bending moment, without upsetting the unit of Stress.

Thus, Equation 12 can be considered the stress equation, to convert the bending moment endured by an SPR in the car body into its corresponding critical stress. The critical stress created can then be used to estimate fatigue life using a stress life curve of the joint.

6.4 Derivation of stress equation for 3-9 failure

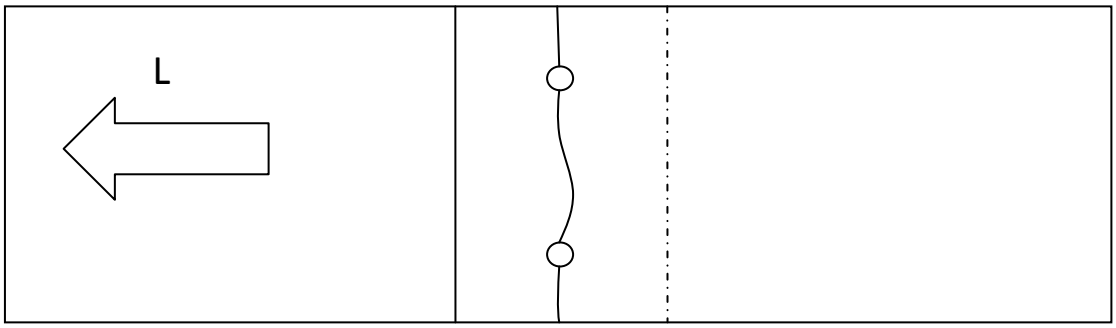

Figure 51: 3-9 failure mode in lap shear configuration

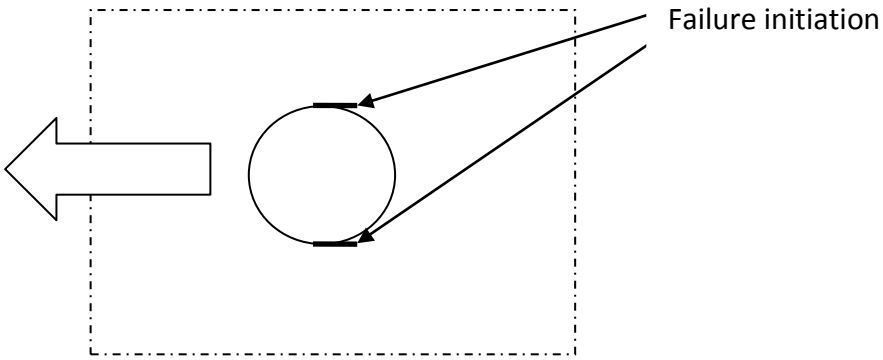

Figure 52: Failure initiation induced by pure shear force

The failure initiation locations are diametrically opposite to each other as shown in Figure 52, as also mentioned in section 2.2.2 and section2.3.3 of chapter 2. As mentioned in chapter 2, it may be assumed that the stresses induced at locations of failure initiation at the top sheet are due to pure shear force tending to shear the rivet out of the stack. And, considering top sheet failure, the stress can be expressed as Force/Area under shear as follows:

$$\sigma = \frac{2.D_{f2}.L}{S_1.\pi.d}$$

Equation 13 : Conversion of shear force to stress (proposed model)

Where,

d= rivet diameter,

D_{f2} = Second deformation factor and

L= applied shear load

The above equation is derived by taking into account the two areas under stress at locations diametrically opposite to each other in the top sheet (Figure 53). Each area is considered to be the multiplication of the top sheet thickness (considered due to failure of top sheet) and quarter of the perimeter of the circle with diameter equal to the rivet diameter. Stress is calculated as force upon sum of the two areas.

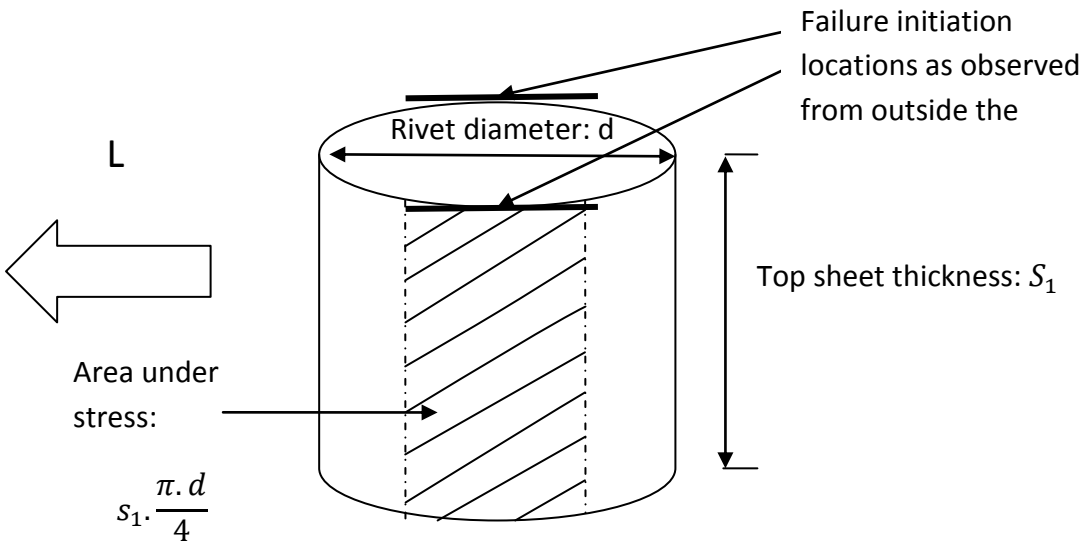

Figure 53: Area under stress due to pure shear load

Thus, Equation 13 may be considered the stress equation for converting shear forces that an SPR endures in a car body, into its corresponding critical stress. The life of the joint can then be estimated, using the stress life curve.

6.5 Working methodology

A simplified conceptual methodology for the working of the new model can be summarised as the following steps:

1. Identifying the key fatigue failure modes and mechanisms that are specific to SPR joining aluminium panels, through study of appropriate laboratory tests.

2. Deriving equations that convert applied force on the joint to its corresponding critical stresses, at the failure initiation locations based on an understanding of the key failure mechanisms.

3. Generating a force life curve based on lab fatigue tests of the joint samples

4. Converting the force life curve into its corresponding stress life curves based on the equations developed

5. Using FE to identify the forces and moments that pass through the critical joints in the car body. Converting the forces and moments into its corresponding stresses, and based on equations derived in step two using a fatigue estimation software, and matching them against the stress life curve generated at step four to estimate the life of the joint.

It may be noted again, that there may be many complexities involved with the fatigue estimation spot joints in car body structure. The steps mentioned above are a basic conceptual structure for the model.

6.6 Stress-life curve

Based on the equations derived above, a stress-life curve using the joints fatigue tested at Coventry University (as mentioned in chapter 2) may be arrived at as follows:

The following table details the results of the fatigue tests:

Life	LoadAmp	failure type
1631987	2.7	eyebrow
1548976	2.7	eyebrow
133476	5	eyebrow
112994	5	eyebrow
137421	5	eyebrow
54228	7.2	SC
62763	7.2	SC
51127	7.2	SC

Figure 54: Coventry University fatigue test data

For eyebrow failure assuming:

D_{f1}= 1,

M= same as the magnitude of the applied load

S1 (top sheet thickness): 2 mm

S2 (bottom sheet thickness): 3 mm

b (sample width): 6 cm

And, for Stress Concentration (3-9) failure, assuming:

D_{f2}= 1

D(rivet diameter) = 6 mm

Using Equation 12 for eyebrow failure and Equation 13 for 3-9 failure, the Stress-life table shown in Figure 55 is generated. The stress-life curve shown in Figure 56:

Stress Mpa	Life cycles
1632	1631987
1549	1548976
133	133476
113	112994
137	137421
54	54228
63	62763
51	51127

Figure 55: Coventry University fatigue tests - stress life table

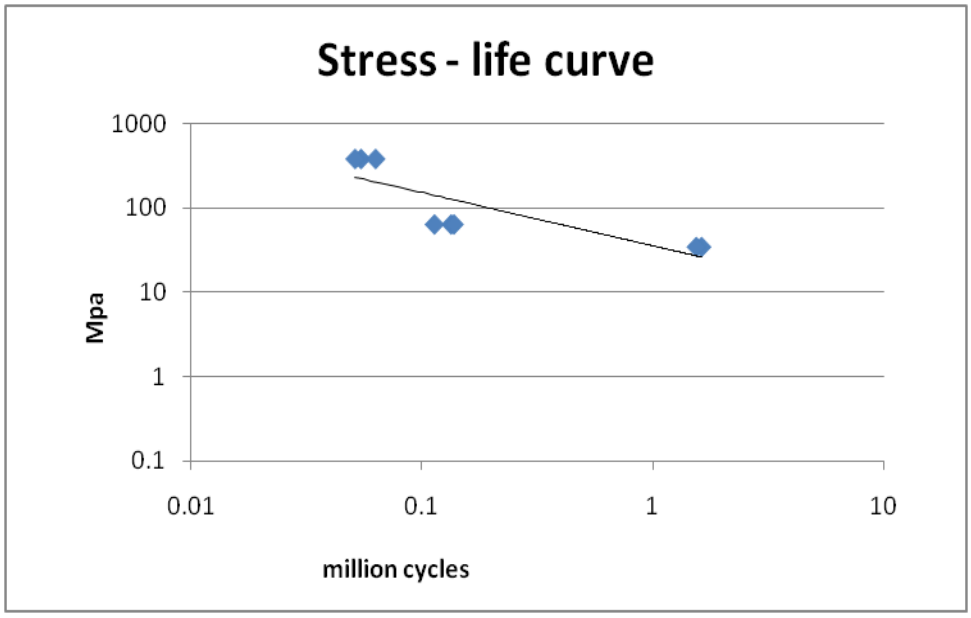

Figure 56: Stress-life curve using Coventry University fatigue tests

6.7 Key features of the model

1. The model has been developed based on the general perception that the joints in the car body are designed in a manner that they mostly endure shear load. Based on

this perception, the model has been developed around the behaviour of SPR joints in the lap shear fatigue test configuration.

2. The model has been built around two most observed fatigue failure mechanisms, i.e. the eyebrow failure mechanism and the 3-9 failure mechanism.

3. Of the two failure modes mentioned above, the eyebrow failure mode is the more commonly observed failure mode. Equation 12 is will be brought to use for low to medium loads, where the joint tends to endure some bending. Whereas, Equation 13 will be brought into use when the joint undergoes heavy load cycles.

4. For the eyebrow failure mode, the model considers the bending moment induced at the joint location, for the calculation of critical stress.

5. The model considers a pure shear (shear only) force for critical stress calculation for a 3-9 failure.

6. In the eyebrow failure mode there is evidence of fretting damage at the bent sheet-sheet interface. Shear stress is considered as the key parameter for initiation of fretting fatigue failure. Therefore, an adaptation of the 'shear stress due to bending' equation takes into account the fretting factor.

7. The model takes into account the proximity of joints to each other by considering the load transferred through the cross sectional area of the sheet stack. The cross sectional area considered for failure, is the area in close proximity to a single rivet. The cross sectional area considered for failure will increase as the distance between rivets increase, i.e. the value b in Equation 12 will increase, as the distance between

rivets increase. Therefore, design engineers can study the effect on rivet proximity on the fatigue life of the body structure, by adjusting the value of b.

6.8 Key improvements

The key improvements of the model when compared with the gaps highlighted in Chapter 5 can be expressed concisely as follows:

1. The Dannbauer model for SPR fatigue estimation does not consider SPR fatigue failure mechanisms. The proposed model is on observed SPR fatigue failure mechanisms.

2. In the Dannbaur model no attempt has been made to capture the failure mechanisms and the reliance is heavily and only on test data. As mentioned in chapter 5, such a dependence on test data would mean the model would move towards being less valid when the car body endures situations alien to laboratory conditions in which the tests were conducted. In the proposed model, along with the test data, a use of the understanding of SPR fatigue failure mechanisms would give the model more confidence in the estimation process.

3. The evidence of fretting was found at the critical location of SPR fatigue failure as mentioned in previous chapters. Existing models for fatigue estimation of SPR in automotive structures do not factor in the effect of fretting fatigue. The proposed model takes into account the fretting factor, through the computation of shear stress at the critical location.

4. The existing models inadvertently assume a joint as being located in an infinite plane, through its calculation processes which are done on individual joints. The

proposed model takes into account the load sharing between joints. The sample width factor 'b' in Equation 12 is directly proportional to the distance between adjacent joints. According to the equation, the stress would increase as a result of a greater distance between joints. Design engineers can adjust the value of 'b' and study its corresponding effect on the stress. In stress life curves derived by testing samples with a single joint, the value 'b' will be the width of the cross sectional panel, the load transfer through which is withstood by one joint.

6.9 Industrial validation process

For the model to be used in the industry, it needs to go through a rigid validation process, and some improvements, adjustments, and changes made along the way.

The industrial validation process for this model, to enable its use in the car industry, may be described in the following steps:

1. Calibration of Equations:

   Calibrating the stress equations for both shear force and bending moments can be done with the stress results from detailed FE analysis of the lap shear joint.

   For equations,

   $\tau = \frac{D_{f1}.12\ .M.{S_1}^2}{b.(S_1+S_2)^3}$ (Equation 12)

   and

   $\sigma = \frac{2.D_{f2}.L}{S_1.\pi.d}$ (Equation 13),

the value of constants $D_{f1.}$, and D_{f2} may be arrived at or adjusted after initial hypothetical assumptions, by using FE to calculate the value to stresses τ, and σ for a given load cycle.

2. Generation of Force-life curve through fatigue tests:

   A force-life curve must be generated based on fatigue tests at different load levels as mentioned in the previous sections.

3. Generation of Stress-life curve:

   The force life curve may then be converted into stress life curve using the calibrated stress equations.

4. Fatigue estimation software:

   The stress life curve and the formulae can then be fed into Fatigue analysis software like HBM ncode Design Life. Mean stress correction may be used based on the test parameters. Other corrections may be introduced based on surface treatment of samples etc. These corrections can be made by the engineer in the Fatigue analysis software.

5. FE analysis of car body:

   The large FE file of car body to be analysed may now be fed into a suitable FE solver. The SPR may be modelled using beam elements. Based on the load cycles applied to the car body, the joints go through two major types of forces:

   a. Shear force

   b. Bending moment

The joints undergoing a transfer of mainly shear forces can have those forces converted to its corresponding stresses using the calibrated Equation 13. And the joints enduring bending moments can have those moments converted into its corresponding stresses using the calibrated Equation 12. The calculations are carried out by the fatigue estimation software.

6. Fatigue life estimation of joints:

   The stresses at the critical joints can now be assigned an estimated life, based on the stress life curve fed into the software database.

7. Body in White testing:

   The car Body in White (BIW) can then be tested with exactly the same signals as the FE input of the car body in the Fatigue analysis software.

8. Comparison and changes:

   The results from the BIW testing and the life estimation provided by the model can then be compared. Improvements and changes may be made accordingly.

6.10 Summary of the chapter

In light of the gaps in knowledge highlighted in chapter 5, in this chapter a new model for fatigue estimation of SPR in aluminium car body was proposed. There is no numerical model in literature for the fatigue estimation of SPR joints in car body that is based on the failure mechanism of SPR. The Dannbauer model relies exclusively on laboratory test data in terms of fatigue life to account for all possible fatigue behaviours of SPR. Improvisations are also made by the Dannbauer model in the modelling of joints, to represent SPR. The Rupp model

represents the behaviour of spot welds. The proposed model is based on stress life methodology. It also takes into account the fact that the failures in SPR joints joining aluminium panels, is predominantly a failure in the sheets stack. Two major failure modes are considered – the eyebrow failure, and the stress concentration failure. The fretting factor present in SPR joints is also taken into account. The model also takes into account the proximity between joints. Equations were derived to convert the shear force and bending moment endured by joints in the car body, into its corresponding critical stresses. A stress life curve was developed using the equations derived and the joints tested at Coventry University. A validation plan was laid down for the industry to follow, if the model were to be used in the car industry.

7. Discussion

7.1 Fatigue, its nature and appropriate approximations

Fatigue is the cause for almost 90 % all metal failures according to all major sources. Hence ignoring it is not an option. Any good structural design especially the design of bodies that undergo repeated loading has the fatigue life of the body and its smaller components as a major design criteria. Apart from a robust estimation there is need for educating the design engineer about the nature of fatigue and the calculation methods and processes used in the estimation models, so the engineer can make decisions about the design of the body based on facts. There could be two kinds of a fatigue life estimation models:

1. An empirical model based fully and only on test data.

2. A theoretical or a semi-empirical model based on an understanding of the physics of the failure mechanism.

7.1.1 An empirical model

An empirical model inadvertently attempts to estimate the fatigue life, without an attempt to understanding the intricate physical mechanics through which the failure takes place. Such a model would depend upon a large amount of test data. With this approach the following points are vital for consideration:

1. The test conditions where the data is gathered vis-à-vis the real life condition of the joint on the car body.

2. The appropriate test parameters at which the data may be considered approximately close to representing real life behaviour.

The Dannbauer model discussed in Chapter 2 makes use of this kind of approach. For the design engineer, in the FEMFAT fatigue analysis software package, the appropriate database is accessed for fatigue estimation based on the magnitude and direction/orientation of forces that pass through the joint in the car body.

Possible disadvantages:

1. The development of such a model is not cost effective and efficient due to large number of fatigue tests that will need to be done to develop a reliable database.

2. The huge number of fatigue tests would mean that the tests need to be done at different facilities, which could induce greater variability in the data due to various uncontrollable noise factors.

Possible advantages:

1. Owing to the probabilistic nature of the fatigue phenomenon, it could be argued that greater the amount of data the greater the reliability.

2. It could also be said that not relying on the theoretical assumptions could be an advantageous prevention against possible theoretical errors in capturing the complex mechanism of fatigue failure.

7.1.2 A theoretical model

A theoretical model will be based on an understanding of the fatigue failure mechanisms observed in laboratory tests. chapter 2 details the observed and documented fatigue failure modes and mechanisms. Theoretical models are generally used in combination with test data.

Possible disadvantages:

1. It could be argued that trying to capture the physics of a probabilistic phenomenon like fatigue failure of SPR could be erroneous. The model inadvertently considers a limited number of failure mechanisms and tries to simplify them and define them with mathematical equations. However, fatigue of a complex joint like SPR could have more failure mechanisms than what could possibly be studied, understood and built into a model.

2. Reduction in the quantity of test data has advantages with respect to cost and reduction in variability. However, it could be argued to be disadvantageous as a greater pool of data, could be argued as adding to the robustness of the model.

Possible advantages:

1. It could be argued that an understanding of the physics of the failure mechanism would enable more adaptability toward real life conditions which is different from laboratory test conditions.

2. It could effectively cut down the total number of fatigue tests necessary to build the model thus reducing the cost, variability and inconsistencies that could arise from conducting a large number of fatigue tests in potentially different locations.

The Rupp model mentioned in Chapter 4 is theoretical or semi-empirical models. The model proposed in this thesis in Chapter 6 is also a theoretical or semi-empirical model, as it needs to be used along with test data.

7.2 Determination Vs Estimation

The common practice among design engineers is to give fatigue a deterministic number during the design of the car body. However, in reality, fatigue as a phenomenon can only be estimated. Therefore, giving it a deterministic number, albeit considered the only way of contemplating fatigue during design, may well be argued as erroneous. Such largely prevalent design practice can also be arguably associated with any eventual over design, arising out of a limited understanding of the phenomenon. Therefore, it is important for the design engineers to appreciate the probabilistic nature of fatigue in order for appropriate design. There might be a need to improvise or even challenge the prevalent design practices in light of a better understanding of fatigue, if significant advances are to be made, in terms of reducing over engineering without compromising safety.

7.2.1 Fatigue analysis methodology - design engineer's point of view

The HBM ncode Designlife fatigue analysis package is considered in this section in order to understand the prevalent mindset among design engineers who analyse car bodies for fatigue:

Designlife package enables the engineers to contemplate fatigue during design, in the following manner. It suggests that the designers make use the unique '5 box' method. The 5 boxes are:

1. Geometry of the body
2. Loading
3. Material properties
4. Spot joint fatigue calculations
5. Output/result

It may be noted again that:

- The above mentioned method is the basic structure or logic of how design life teaches designers to estimate fatigue. Complexities arise as complex geometries and various other design considerations are added to the process. However, the basic structure or logic of the methodology remains similar.
- Even though the issues discussed in this section apply as such to fatigue as phenomenon, the analysis is done in the context of spot joints – namely Self Piercing Rivets. Therefore, a lot of the arguments will hold true only as far as fatigue analysis of Self Piercing Rivets in car body is concerned.

Geometry of the body:

This box considers of the geometry of the car body. According to the geometry, the external forces that are applied to the car body, are broken down into various individual force vectors that pass through the spot joints.

Loading:

This box takes into account the loads or forces that the car body is subjected to. The fatigue behaviour of any component or material varies significantly according to the load that the body is subjected to.

Material Properties:

This box takes into account the material properties of the parts or components that are joint together. Fatigue behaviour varies heavily according material property.

Spot joint fatigue calculations:

This box consists of the actual empirical or semi-empirical model for fatigue estimation of spot joints. Inputs from the previous boxes are fed into it. Fatigue estimations for each of the joints are fed onto the output box after calculations.

Output box:

This is the box that engineers use as a reference for their design considerations. The output from the calculations box is fed into this box to be displayed to the engineers, for further design analyses.

A simple illustration of fatigue estimation using DesignLife is shown in the Figure 57 below. The basic building blocks used in this fatigue analysis software as seen in Figure 57 are termed as glyphs. The 'FEInput1' glyph deals with the geometry of the body. The 'TSInput1' glyph represents the loading pattern on the body, or the forces the body is subjected to. The 'SpotWeldAnalysis1' glyph consists of the material properties, and the calculations for fatigue estimation. And, the 'FEDisplay1' glyph represents the load cycles that the spot joints endure based on the calculation, or the fatigue life of the spot joints.

Figure 57: Fatigue analysis – design engineer's window (ncode, 2009)

There are many other glyphs that can be used in studying and analysing the fatigue calculations, like the metadata display glyph shown in the figure below.

Figure 58: Example of a deterministic output of fatigue life (HBMncode, 2009)

As seen in Figure 58, the fatigue life is given to the design engineer as a deterministic value.

Most other commercial fatigue estimation packages follow a similar methodology.

7.2.2 The range of fatigue life

It may be argued that, all the rigour and precision that goes into estimating a fatigue life, essentially goes to waste by giving it a rigorous value, because it might never be the right number, as there is no right number in fatigue. As, at any given load level or stress level, fatigue life consists of a range of numbers in reality, even though the design engineer just gets one number. It may be argued that the design engineers get the mean of the range of numbers, which is a fairly estimated number. However, it would again lean on the assumption that, the mean number is the most likely number that the failure will pick. It is no different from a school inspector being expected to randomly pick up a student with the mean score of the class in a test. What design engineers should ideally get, after due training and education, is the whole range of numbers that the fatigue failure can pick from, for each joint that is analysed.

7.3 Reliability of Experimental data (R and R)

In an effort to understand fatigue, there are attempts made to capture the source of variations or scatter in fatigue. In the development of an empirical or semi empirical fatigue estimation model, there is a data generation process involved. Samples are fatigue tested for the generation of this data. Generally during any data generation there is a Repeatability and Reproducibility (R and R) technique applied. The probabilistic nature of fatigue makes an R and R study to improve the data generation process all the more important. It is done for the following main purposes:

- To assess or study the measurement systems and the data generation systems and processes in general.
- To try and understand precisely, the sources of variation or scatter in the test data.
- Try and minimise the scatter as much as possible.

This is carried out in order to generate what is believed as a better quality, more representative, and more useful data.

7.3.1 Use of P diagram

The P diagram is a tool used to view the various parameters affecting a system's ideal output state. During data collection for fatigue analysis, P diagram is used to work towards generating better quality data.

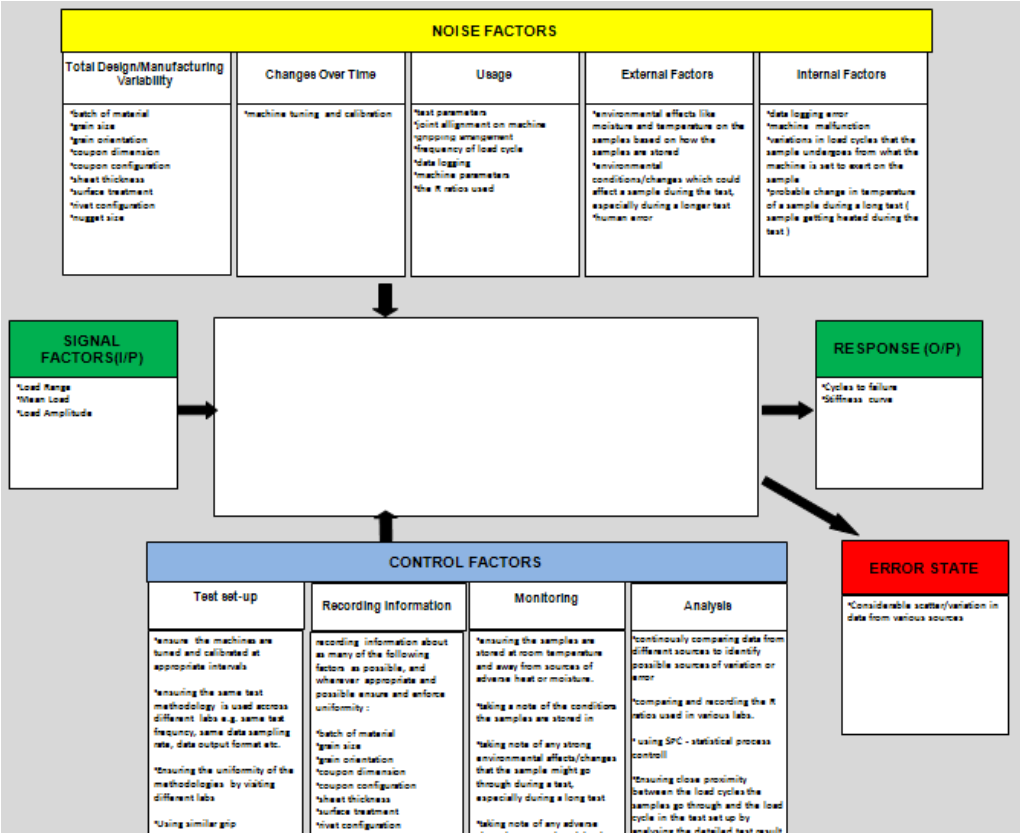

Figure 59: P diagram

Figure 59 shows a P diagram. The P diagram for data generation for fatigue tests consists of the following components:

1. Noise factors:

   These constitute the factors that would tend to induce the 'error state' in a system of perfect data generation.

2. Control factors:

These factors include the measures that could be taken to minimise and hypothetically negate the 'error state'.

3. Error state:

   This is the state where the inputs given into the system, get affected by the noise factors and account for considerable variation and scatter in the data.

Noise Factors:

In a data generation system, consisting of multiple labs, the noise factors could be categorized as:

1. Design and manufacturing variability:

   This includes batch of materials, grain size, grain orientation, coupon dimension, coupon configuration, sheet thickness, surface treatment, rivet configuration, nugget size etc.

2. Changes over time:

   This includes changes in machine tuning and calibration.

3. Usage:

   Different usages could include, different test parameters, different joint alignment on different machines, gripping arrangement differences, frequency of load cycle, data logging differences, machine parameter uniqueness, and difference in R ratios.

4. External factors:

External factors include effect of environmental factors like moisture and temperature on how samples are stored, change in environmental factors during the course of a test, human error etc.

5. Internal factors:

   Internal factors include data logging errors, machine malfunction, variations in set load cycles, and possible change in temperature of the sample during the test.

To try and minimise the effect of these factors, there exists another constituent of the p diagram called the 'Control factors'.

Control factors:

They consist of the following:

1. Test set-up:

   This includes:

   - Ensuring the machines are tuned and calibrated at appropriate intervals
   - Ensuring the same test methodology is used across different labs
   - Ensuring the uniformity of various labs through inspection
   - Using standard or at least similar grip arrangements to ensure correct alignment.

2. Recording all information:

This includes recording as many information as possible, and wherever appropriate and possible ensure uniformity in: batch of material, grain size, grain orientation, coupon dimension, coupon configuration, sheet thickness, surface treatment, rivet configuration, nugget size etc.

3. Monitoring:

   This includes:

   - Ensuring the samples are stored at room temperature and away from sources of adverse hear and moisture.
   - Taking a note of conditions that samples are stored in.
   - Taking note of any strong environmental affects/changes that the sample might go through during a test, especially during a long test.
   - Taking note of any adverse signs that a sample might show during a test, e.g. adverse change in temperature, deformation etc.

4. Analysis:

   This includes:

   - Continuously comparing data from different sources to identify possible sources of variation or error
   - Comparing and recording the R ratios used in various labs
   - Using statistical process control

- Constantly analysing test results to ensure load cycles follow the right patterns.

However, despite all these efforts to reduce scatter, it may be argued that in fatigue scatter could be seen as something more representative of reality rather than something undesirable which needs to be minimised in an effort to hypothetically eliminate it.

7.4 Comparison

Following is a brief summary of the comparisons made between the proposed SPR fatigue estimation model, and the existing fatigue estimation models suited for SPR in the thesis.

7.4.1 Fretting

Fretting is an important phenomenon that exists in the fatigue behaviour of SPR. The phenomenon of fretting generally has a detrimental effect on the fatigue of components that it affects. The Dannbauer model, and the Rupp model, does not factor in the phenomenon of fatigue. The proposed model, considers shear stress in the failure initiation location, as the failure criterion. Shear stress in critical plain is considered as fretting failure initiation criteria. Thus, the proposed model factors in fretting fatigue, for the eyebrow failure mode, which is the dominant failure mode.

7.4.2 Bending

Joints under shear loading in low to medium load levels undergo a bending. The proposed model comprises of a combination of bending and fretting as discussed in Chapter 6. The Dannbauer model does not take into account any observed SPR failure mechanisms. The Rupp model does take into account the bending moment, and converts it into its

appropriate stress. However, it considers a spot weld for the derivation of the stress equations. Also, it does not factor in fretting fatigue.

7.4.3 Shear force

Joints under shear loading at high load levels have a dominant shear component of force than the induced bending. The Dannbauer model does not factor this effect. The Rupp model does factor the effect of shear force. However, the stress equations are derived in light of spot weld fatigue behaviour which differ from SPR. The proposed model derives an equation based on the 3-9 failure, which the joint undergoes under heavy load, with the dominant influence of the shear component of the applied force (Equation 13).

7.4.4 Joint proximity and load sharing

To reduce over engineering, a design engineer has to study the effect of the proximity of rivets to each other during the design stage. However, in the existing models, the extra stress induced in a joint in relative isolation compared to a joint in close proximity with other joints, can only be factored in based on the modelling of the joints in the FE model of the car body. In the proposed model, the proximity of rivets to each other, or the area of the cross section covered by the endurance of a single rivet, is directly factored in using the width factor ‘b’ in Equation 12. ‘b’ is directly proportional to the proximity of joints to each other and inversely proportional to the critical stress induced.

7.4.5 Similarities

All models discussed in the thesis for the fatigue estimation of spot joint in the car body, use the stress life methodology. All the models make use of the stress life curves. The Rupp model does use the methodology of converting moments and shear forces into its

corresponding stresses like the proposed model, although it derives different set of equations for the purpose.

8. Conclusion

The thesis could be summarised as follows:

1. A study was made on the different available models and methodologies for the fatigue life estimation of SPR in the aluminium car body.

2. The gaps in knowledge were identified. Gaps exist mainly because SPR is different in fatigue behaviour from the widely used spot welds, and there only exists a numerical model for fatigue estimation of spot welds in car body.

3. A detailed study of various SPR fatigue failure mechanisms was done.

4. A new numerical model was proposed based on the fatigue failure mechanisms of SPR joints. The fretting factor was incorporated. Equations were derived to convert shear force and bending moment into their respective critical stresses, for life estimation using the stress life methodology.

5. A validation plan was laid out for the model to be adapted for use in the industry.

9. Further Work

An immediate further work of this thesis would be a BIW validation like explained in section 6.9, of the proposed model put forth in this thesis. During the validation processes refining of the equations and other improvements may be brought into place. With newer materials and joining processes coming into existence, to ultimately achieve the goal of reducing over-engineering, newer methods and rationales need to be tested and validated. Further improvisations of existing models built primarily for former materials and joining techniques, may only go to a certain point in achieving competent results.

There is also scope for continuous improvement in the following areas:

1. FE modelling of the joints:

   There are different ways in which the joints can be modelled in the FE model of the whole car body. Each method could have its own effect on the forces and moments that would be transferred through it in the fatigue estimation process. A research on the appropriate modelling of these joints could be done so the forces transferred in the FE model through these joints reflect the forces transferred through the joints in the real world as closely as possible.

2. FE calibration of equations:

   A robust and detailed FE model may be created and used not only to calibrate the stress equations using the various options available in FE packages but also to study the SPR behaviour even further.

3. Test data generation, analysis and formatting:

The reliability of the test data is indispensable for any fatigue estimation model. Work could be done on developing a methodology for greater reliability in data acquisition and analysis. This is important especially due to the requirement of a large volume of test data and possible multiple locations for their generation. A data generation project may have noise factors like machine parameters, sample alignment on the machine, test parameters, material batch and some environmental conditions specific to the lab. Some noises may be relatively easier to bring under control than the others.

4. Test sample configuration:

   The test sample configuration could have a significant effect both on the fatigue failure mechanism as well as the total fatigue life of sample. Therefore, a research could be done on developing a configuration that would best replicate the real life.

5. Fatigue estimation software technicalities:

   It is the fatigue estimation software that the design engineer ultimately uses in order to design an efficient and robust car. Therefore the technical capabilities of the software will have an impact on facilitating the design process. Work could be done on formatting the data appropriately for an efficient and effective use of the fatigue estimation tool. The access to the original range of data and methods of calculation could arguably enable the design engineer to make a better decision. There is benefit in making a fatigue estimation tool more efficient, open and easy to use.

References

ABE, Y., KATOB, T. & MORIA, K. (2009) Self-piercing riveting of high tensile strength steel and aluminium alloy sheets using conventional rivet and die. *journal of materials processing technology 209***,** 3914–3922.

AGRAWAL, H., LI, W., BOLLIMUNTA, S., POTTY, K. & BLOWS, A. (2003) Fatigue Life of Self Pierced Rivets (SPR) in Car Body. *SAE TECHNICAL PAPER SERIES*.

ATZENI, E., IPPOLITO, R. & SETTINERI, L. (2009) Experimental and numerical appraisal of self-piercing riveting. *CIRP annals - Manufacturing Technology,* 342.

BISHOP, N., W, M & SHERRATT, F. (2000) *Finite Element based Fatigue Analysis*.

BLACKMORE, P. (2007) Fatigue Damage Mechanisms in SPR joints. Jaguar Cars Ltd.

BRISKHAM, P., BLUNDELL, N., HAN, L., HEWITT, R., YOUNG, K. & BOOMER, D. (2006) Comparison of Self-Pierce Riveting, Resistance Spot Welding and Spot Friction Joining for Aluminium Automotive Sheet.

BUCIUMEANU, M., CRUDU, I., PALAGHIAN, L., MIRANDA, A. S. & SILVA, F. S. (2008) Influence of wear damage on the fretting fatigue life prediction of an Al7175 alloy. *International Journal of Fatigue,* 31**,** 1278-1285.

CADARIO, A. & ALFREDSSON, B. (2005) Fretting fatigue crack growth for a spherical indenter with constant and cyclic bulk load. *Engineering Fracture Mechanics,* 72**,** 1664-1690.

CALLISTER, W., D. (2007) *Materials Science and Engineering An Introduction* John Wiley and Sons, Inc.

CASALINO, G., ROTONDO, A. & LUDOVICO, A. (2008) On the numerical modelling of the multiphysics self piercing riveting process based on the finite element technique. *Advances in Engineering Software,* 39**,** 787–795.

CHEN, Y. K., HAN, L., CHRYSANTHOU, A. & O'SULLIVAN, J. M. (2003) Fretting wear in self-piercing riveted aluminium alloy sheet.

DANNBAUER, H., GAIER, C. & HALASZI, C. (2003) Development of a Model for Self-piercing Rivts to Predict Stiffness and Fatigue Life of Automotive Structures.

DE-GUANG, S., WEI-XING, Y. & DE-JUN, W. (1998) A new approach to the determination of fatigue crack initiation size. *International Journal of Fatigue,* 20**,** 683-687.

DONDERS, S., BRUGHMANS, M., HERMANS, L., LIEFOOGHE, C., VAN DER AUWERAER, H. & DESMET, W. (2006) The robustness of dynamic vehicle performance to spot weld failures. *Finite Elements in Analysis and Design,* 42**,** 670-682.

ELKHOLY, A. H. (1996) Fretting fatigue in elastic contacts due to tangential micro-motion. *Tribology International,* 29**,** 265-273.

FADAG, H. A., MALL, S. & JAIN, V. K. (2008) A finite element analysis of fretting fatigue crack growth behavior in Ti-6Al-4V. *Engineering Fracture Mechanics,* 75**,** 1384-1399.

FATEMI, A. & ZOROUFI, M. (2005) Automotive forgings and fatigue: a research paper. *Designfax.* Euenterpreur connect.

FERMÉR, M., MCINALLY, G. & SANDIN, G. (1999) Fatigue Life Analysis of Volvo S80 Bi-Fuel. *1st Worldwide MSC Automotive Conference.* Munich, Germany, Volvo Car Corporation, SE-405 08 Göteborg, Sweden.

FU, M. & MALLICK, P. K. (2001) Effect of Process Variables on the Static and Fatigue Properties of Self-Piercing Riveted Joints in Aluminum Alloy 5754. *SAE TECHNICAL PAPER SERIES*.

GARCIA, D. B. & GRANDT, A. F. (2007) Application of a total life prediction model for fretting fatigue in Ti-6Al-4V. *International Journal of Fatigue,* 29**,** 1311-1318.

GOKHALE, N., S, DESHPANDE, S., S, BEDEKAR, S., V & THITE, A., N (2008) *Practical Finite Element Analysis*, Finite to Infinite, Pune.

GRAEVE, I., DE & ZENGEN, K.-H., VON (2009) Aluminium in car body - Introduction 1. *Alumatter.* European Aluminium Association

University of Liverpool.

GRINBERG, N. M. (1984) Stage II fatigue crack growth. *International Journal of Fatigue,* 6**,** 229-242.

HAMANO, R. (1997) Fatigue crack growth from stage I to stage II in a corrosive environment. *International Journal of Fatigue,* 19**,** 197-204.

HAN, L. & CHRYSANTHOU, A. (2007) Evaluation of quality and behaviour of self-piercing riveted aluminium to high strength low alloy sheets with different surface coatings. *materials and design*.

HAN, L., HEWITT, R., SHERGOLD, M., CHRYSANTHOU, A. & STEPINSKI, T. (2007) An Evaluation of NDT for Self-pierce Riveting. *SAE TECHNICAL PAPER SERIES*.

HAN, L., YOUNG, K., W, HEWITT, R., ALKAHARI, M., R & CHRYSANTHOU, A. (2006) Effect of Sheet Material Coatings on Quality and Strength of Self-Piercing Riveted Joints. *SAE TECHNICAL PAPER SERIES*.

HBMNCODE (2009) Glyphworks worked example.

HE, X., PEARSON, I. & YOUNG, K. (2008) Self-pierce riveting for sheet materials: State of the art. *journal of materials processing technology - 199***,** 27–36.

HELMUT, D., GAIER, C. & HOFWIMMER, K. (2004) Fatigue Analysis of Welding Seams and Spot Joints in Automotive Structures. SAE.

HERRMANN, P., TING, T. & KITSOSIS, V. (2005) Development of a Fatigue Analysis Tool Chain for Automative Structural Application. *SAE TECHNICAL PAPER SERIES,* 01.

HEYES, P. & FERMER, M. (1996) A spot-weld fatigue analysis module in the MSC/Fatigue environment. MSC.

IYER, K. (2001) Peak contact pressure, cyclic stress amplitudes, contact semi-width and slip amplitude: relative effects on fretting fatigue life. *International Journal of Fatigue,* 23**,** 193-206.

IYER, K., HU, S., J, BRITTMAN, F., L, WANG, P., C, HAYDEN, D., B & MARIN, S., P (2005) Fatigue of single- and double-rivet self-piercing riveted lap joints. *FFE***,** 9.

JOHNSON, P., CULLEN, J., D, SHARPLES, L., SHAW, A. & AL-SHAMMA'A, A., I (2009) Online visual measurement of self-pierce riveting systems to help determine the quality of the mechanical interlock. *Measurement* 42 661–667.

KANG, H. & BARKEY, M. E. (1999) Fatigue life estimation of spot welded joints using an interpolation/extrapolation technique. *International Journal of Fatigue,* 21**,** 769-777.

KANG, H. T. (2007) Fatigue prediction of spot welded joints using equivalent structural stress. *Materials & Design,* 28**,** 837-843.

KELKAR, A., ROTH, R. & CLARK, J. (2001) Automotive Bodies: Can aluminium be an economical alternative to steel. *Journal of Automobile Materials,* 53**,** 28-32.

LIGUORE, S., L & BEIER, T., H (2001) Recognition and Correction of Sonic Fatigue Damage in Fighter Aircraft. Manchester.

LYKINS, C. D., MALL, S. & JAIN, V. (2001) A shear stress-based parameter for fretting fatigue crack initiation. *Fatigue & Fracture of Engineering Materials & Structures,* 24**,** 461-473.

MANSON, S., S & HALFORD, G., R (2006) *Fatigue and Durability*, ASM International, USA.

MUÑOZ, S., NAVARRO, C. & DOMÍNGUEZ, J. (2007) Application of fracture mechanics to estimate fretting fatigue endurance curves. *Engineering Fracture Mechanics,* 74**,** 2168-2186.

MUÑOZ, S., PROUDHON, H., DOMÍNGUEZ, J. & FOUVRY, S. (2006) Prediction of the crack extension under fretting wear loading conditions. *International Journal of Fatigue,* 28**,** 1769-1779.

NAVARRO, C. & DOMÍNGUEZ, J. (2004) Initiation criteria in fretting fatigue with spherical contact. *International Journal of Fatigue,* 26**,** 1253-1262.

NAVARRO, C., GARCÃ□A, M. & DOMÃ□NGUEZ, J. (2003) A procedure for estimating the total life in fretting fatigue. *Fatigue & Fracture of Engineering Materials & Structures,* 26**,** 459-468.

NAVARRO, C., MUÑOZ, S. & DOMÍNGUEZ, J. (2008) On the use of multiaxial fatigue criteria for fretting fatigue life assessment. *International Journal of Fatigue,* 30**,** 32-44.

NCODE, H. (2009) Design Life Worked Examples 6.

NEU, R. W. (2008) The fretting fatigue behavior of Ti-6Al-4V. *Key Engineering Materials,* 378379**,** 147-162.

PAPAZIAN, J. M., NARDIELLO, J., SILBERSTEIN, R. P., WELSH, G., GRUNDY, D., CRAVEN, C., EVANS, L., GOLDFINE, N., MICHAELS, J. E., MICHAELS, T. E., LI, Y. & LAIRD, C. (2007) Sensors for monitoring early stage fatigue cracking. *International Journal of Fatigue,* 29**,** 1668-1680.

RUPP, A., STIJRZEL, K. & GRUBISIC, V. (1995) Computer Aided Dimensioning of Spot-Welded Automotive Structures. *SAE TECHNICAL PAPER SERIES*

SANTUS, C. & TAYLOR, D. (2008) Physically short crack propagation in metals during high cycle fatigue. *International Journal of Fatigue,* 31**,** 1356-1365.

SHIBATA, K., IWASW, T., SAKAMOTO, H. & KASUKAWA, M. (2003) Welding of aluminium car boy parts with twin-spot high power Nd: YAG laser *Welding international,* 17**,** 939-946.

SOCIE, D. F., MORROW, J. & CHEN, W.-C. (1979) A procedure for estimating the total fatigue life of notched and cracked members. *Engineering Fracture Mechanics,* 11**,** 851-859.

STEPHENS, R., I, FATEMI, A., STEPHENS, R., R & FUCH, H., O (2001) *Metal Fatigue in Engineering*, John Wiley and Sons Inc. .

SUM, W. S., WILLIAMS, E. J. & LEEN, S. B. (2005) Finite element, critical-plane, fatigue life prediction of simple and complex contact configurations. *International Journal of Fatigue,* 27**,** 403-416.

SUN, X., STEPHENS, E. V. & KHALEEL, M., A (2006) Fatigue behaviors of self-piercing rivets joining similar and dissimilar sheet metals. *International Journal of Fatigue,* 29.

SURESH, S. (2004) *Fatigue of materials,* Cambridge, Cambridge Univ. Press.

VAZQUEZ, J., NAVARRO, C. & DOMINGUEZ, J. (2010) On the estimation of fatigue life in notches differentiating the phases of crack initiation and propagation. *Fatigue & Fracture of Engineering Materials & Structures,* 33**,** 22-36.

VERDU, C., ADRIEN, J. & BUFFIÈRE, J. Y. (2008) Three-dimensional shape of the early stages of fatigue cracks nucleated in nodular cast iron. *Materials Science and Engineering: A,* 483-484**,** 402-405.

XUE, Y., MCDOWELL, D. L., HORSTEMEYER, M. F., DALE, M. H. & JORDON, J. B. (2007) Microstructure-based multistage fatigue modeling of aluminum alloy 7075-T651. *Engineering Fracture Mechanics,* 74**,** 2810-2823.

YANG, J., LI, Y., LI, S., MA, C. & LI, G. (2001) Simulation and observation of dislocation pattern evolution in the early stages of fatigue in a copper single crystal. *Materials Science and Engineering A,* 299**,** 51-58.

ZHANG, Y. & TAYLOR, D. (2001) Optimization of spot-welded structures. *Finite Elements in Analysis and Design,* 37**,** 1013-1022.

Appendix

1. The Rupp model
2. The Dannbauer model
3. A shear stress-based parameter for fretting fatigue crack initiation

These appendices have been removed as they are published papers. The unabridged version of the thesis can be viewed at the Lanchester Library, Coventry University